




SCALING OF PRESSURE AND SUBCOOLING FOR COUNTERCURRENT FLOW

QUARTERLY PROGRESS REPORT
April 1, 1978 - June 30, 1978

P. H. Rothe
C. J. Crowley

Creare, Inc.
Hanover, New Hampshire

7812180171

 Prepared for
U. S. Nuclear Regulatory Commission

NOTICE

This report was prepared as an account of work sponsored by an agency of the United States Government. Neither the United States Government nor any agency thereof, or any of their employees, makes any warranty, expressed or implied, or assumes any legal liability or responsibility for any third party's use, or the results of such use, of any information, apparatus product or process disclosed in this report, or represents that its use by such third party would not infringe privately owned rights.

Available from
National Technical Information Service
Springfield, Virginia 22161
Price: Printed Copy \$5.25 ; Microfiche \$3.00

The price of this document for requesters outside of the North American Continent can be obtained from the National Technical Information Service.

SCALING OF PRESSURE AND SUBCOOLING
FOR COUNTERCURRENT FLOW

Quarterly Progress Report
April 1, 1978 - June 30, 1978

Paul H. Rothe
Christopher J. Crowley

Manuscript Completed: October 1978
Date Published: October 1978

CREARE Inc.
Hanover, NH 03755

Division of Reactor Safety Research
Office of Nuclear Regulatory Research
U.S. Nuclear Regulatory Commission
Under Contract No. NRC-04-75-162

ABSTRACT

Recent results of a continuing program to develop semi-empirical models of lower plenum filling after a hypothetical PWR LOCA are presented. The idealized situation of countercurrent flow in a 1/15-scale PWR model is specifically addressed here. For saturated water behavior in small-scale facilities, it is shown that the dimensionless J^* parameters properly scale the effects of vessel size, injection rate, and (for the first time with steam and water) vessel pressure. Building on previous work, new correlation concepts are proposed to account for the effects of condensation on ECC bypass. Comparison with new data over an increased range of pressures and subcoolings shows that for a given injection rate, the effects of condensation can be accounted solely in terms of thermodynamic ratio rather than pressure or subcooling independently. The data indicate that subcooling has a weaker effect on ECC bypass than was previously believed. The data also reveal a transition in behavior at a thermodynamic ratio near unity; at values below this transition the behavior is close to that of saturated water at all pressures tested. These findings suggest a need for caution when taking credit for the benefits of subcooling on ECC bypass in calculated LOCA transients.

TABLE OF CONTENTS

	<u>Page</u>
ABSTRACT	iii
TABLE OF CONTENTS	v
LIST OF FIGURES	vii
NOMENCLATURE	x
PREFACE	xi
1 INTRODUCTION	1
1.1 General Background	1
1.2 Countercurrent Flow Studies	1
1.3 Summary of This Report	3
2 CONTEXT OF PREVIOUS RESEARCH	5
3 CORRELATION OF PRESSURE AND SUBCOOLING EFFECTS	8
3.1 The Countercurrent Flow Correlation	8
3.2 Creare Saturated Water Data	10
3.3 Creare Data for Effects of Condensation	12
3.4 Comparisons With Additional Creare Data	12
3.5 Correlation Methods	19
4 PROGRESS ON SCALING OF COUNTERCURRENT FLOW	27
4.1 Scaling of Saturated-Water Behavior	27
4.2 Preliminary Scaling Assessment of Subcooled Water Data	31
5 SUMMARY OF SPECIFIC FINDINGS ON COUNTERCURRENT FLOW	37
6 CONCLUDING REMARKS ON IMPLICATIONS OF FINDINGS	40
REFERENCES	41
APPENDIX A -- DETAILED LITERATURE REVIEW	44
A.1 Correlation for Air/Water in Tubes	44
A.2 Correlation of Model Reactor Vessel Geometries	45
A.3 Effects of Thermal and Hydraulic Parameters	49
APPENDIX A REFERENCES	53
APPENDIX B -- COUNTERCURRENT FLOW DATA TABULATION	54

LIST OF FIGURES

<u>Figure</u>		<u>Page</u>
1	POTENTIAL FLOW PATHS FOR A COLD LEG BREAK IN A PWR	2
2	IDEALIZED COUNTERCURRENT FLOW SITUATION	3
3	IDEALIZED ECC BYPASS DATA	6
4	BEHAVIOR OF FACTOR m REPRESENTING PARTIAL DELIVERY	9
5	COMPARISON OF PRESENT CORRELATION WITH CREARE 1/15-SCALE DATA FOR SATURATED WATER AT SEVERAL ECC INJECTION RATES [17]	11
6	COMPARISON OF PRESENT CORRELATION WITH CREARE 1/15-SCALE DATA FOR SATURATED WATER AT SEVERAL VESSEL PRESSURES	11
7	COMPARISON OF PRESENT CORRELATION WITH CREARE 1/15-SCALE DATA FOR SUBCOOLED WATER NEAR AMBIENT PRESSURE [16]	13
8	COMPARISON OF PRESENT CORRELATION WITH CREARE 1/15-SCALE DATA FOR A VESSEL PRESSURE OF 65 PSIA AT VARIOUS ECC SUBCOOLINGS	13
9	COMPARISON OF PRESENT CORRELATION WITH CREARE 1/15-SCALE DATA FOR AN ECC SUBCOOLING OF 135°F AT SEVERAL PRESSURES	14
10	COMPARISON OF PRESENT CORRELATION WITH PRESENT CREARE DATA FOR VARIOUS PRESSURES AND SUBCOOLINGS ARRAYED AS A FUNCTION OF THERMODYNAMIC RATIO	14
11	COMPARISON OF PRESENT CORRELATION WITH EARLIER CREARE 1/15-SCALE DATA FOR 212°F ECC AT SEVERAL INJECTION RATES AND UNCONTROLLED PRESSURES	15
12	COMPARISON OF PRESENT CORRELATION WITH CREARE 1/15-SCALE DATA FOR 45 PSIA VESSEL PRESSURE AT VARIOUS ECC SUBCOOLINGS	16
13	COMPARISON OF PRESENT CORRELATION WITH CREARE 1/15-SCALE DATA FOR 30 PSIA VESSEL PRESSURE AT VARIOUS ECC SUBCOOLINGS	17
14	COMPARISON OF PRESENT CORRELATION WITH CREARE 1/15-SCALE DATA FOR 60°F ECC SUBCOOLING AT VARIOUS PRESSURES	17
15	COMPARISON OF PRESENT CORRELATION WITH CREARE 1/15-SCALE DATA FOR 170°F ECC SUBCOOLING AT VARIOUS PRESSURES	18
16	LIQUID TEMPERATURE IN THE BROKEN LEG OF THE CREARE 1/15-SCALE VESSEL DURING COMPLETE BYPASS	21
17	COMPARISON OF PREVIOUS CORRELATION [13] WITH CREARE 1/15-SCALE DATA FOR SATURATED WATER [17]	22
18	COMPARISON OF PREVIOUS CORRELATION [13] WITH CREARE 1/15-SCALE DATA FOR 135°F ECC SUBCOOLING AT VARIOUS VESSEL PRESSURES	23

LIST OF FIGURES (continued)

<u>Figure</u>		<u>Page</u>
19	COMPARISON OF PREVIOUS CORRELATION [13] WITH CREARE 1/15-SCALE DATA FOR SUBCOOLED WATER AT VESSEL PRESSURES NEAR AMBIENT	24
20	COMPARISON OF CORRELATIONS WITH CREARE 1/15-SCALE DATA SHOWING SENSITIVITY TO FACTORS C AND m	24
21	COMPARISON OF CORRELATIONS WITH CREARE 1/15-SCALE DATA SHOWING SENSITIVITY TO FACTOR f AT AMBIENT VESSEL PRESSURE	25
22	COMPARISON OF CORRELATIONS WITH CREARE 1/15-SCALE DATA SHOWING SENSITIVITY TO FACTOR f AT 65 PSIA VESSEL PRESSURE	26
23	COMPARISON OF CORRELATIONS WITH CREARE 1/15-SCALE DATA SHOWING SENSITIVITY TO FACTOR f FOR 135°F ECC SUBCOOLING	26
24	ECC BYPASS SCALING FOR SATURATED WATER	28
25	COMPARISON OF PRESENT SATURATED WATER CORRELATION WITH BATTELLE 2/15-SCALE DATA [21] SHOWING EXTRAPOLATION TO COMPLETE BYPASS . .	29
26	COMPARISON OF PRESENT CORRELATION WITH BATTELLE 2/15-SCALE DATA [21] FOR NEARLY SATURATED WATER SHOWING WEAK CALCULATED EFFECT OF SUBCOOLING AND INJECTION RATE RELATIVE TO DATA SCATTER	29
27	COMPARISON OF PRESENT CORRELATION WITH DARTMOUTH 1/10-SCALE AIR-WATER DATA [22]	30
28	COMPARISON OF DARTMOUTH 1/10-SCALE AIR-WATER DATA [22] WITH CREARE 1/15-SCALE STEAM-WATER DATA FOR NEARLY SATURATED WATER [17]	30
29	SCALING MAP FOR THE EFFECT OF CONDENSATION ON ECC BYPASS	31
30	COMPARISON OF CREARE DATA AT 1/30 AND 1/15 SCALES FOR HIGHLY SUBCOOLED ECC	33
31	COMPARISON OF BATTELLE DATA FOR STEADY STATE AND PLENUM FILLING TEST MODES AT TWO SCALES	34
32	COMPARISON OF CREARE 1/15-SCALE AND BATTELLE 2/15-SCALE PLENUM FILLING DATA SHOWING DISAGREEMENT OF BOTH WITH BATTELLE STEADY-STATE DATA	35
33	COMPARISON OF 1/15-SCALE DATA FOR PLENUM FILLING AND STEADY-STATE TEST MODES	35
A1	CRITICAL KUTATELADZE NUMBER (DIMENSIONLESS GAS FLUX) BELOW WHICH THE LIQUID FILM WILL FLOW DOWNWARDS	45
A2	COMPARISON OF CCF DATA FOR TWO BREAK SIZES AT 1/15-SCALE	48

NOMENCLATURE

C	correlation factor for saturated water complete bypass (Equation 3)
c_p	specific heat at constant pressure
D	tube diameter
D_h	hydraulic diameter of flow passage
f	correlation factor for effect of condensation on complete bypass (Equation 4)
g	acceleration of gravity
h_{fg}	enthalpy change of vaporization
j	superficial fluid velocity
j^*	dimensionless fluid flux (Equation A5)
J_{fd}^*	dimensionless liquid flux delivered to lower plenum (Equation 2)
J_{fin}^*	dimensionless liquid flux injected
J_g^*	effective dimensionless steam flux for bypass (Equation 4)
J_{gb}^*	dimensionless core steam flux at complete bypass
J_{gc}^*	dimensionless steam flux out of core to lower plenum (Equation 1)
J_{gd}^*	dimensionless core steam flux J_{gc}^* at complete delivery
m	correlation factor for partial delivery (Equation 3)
P_a	atmospheric pressure
P_{LP}	lower plenum pressure
R_T	thermodynamic ratio $\lambda J_{fin}^*/J_{gc}^*$
R_{Tb}	thermodynamic ratio at complete bypass $\lambda J_{fin}^*/J_{gb}^*$
s	annulus gap spacing
T_{ECC}	ECC injection temperature
T_{fb}	liquid temperature in break
T_s	saturation temperature
ΔT_{sub}	ECC subcooling $T_s - T_{ECC}$

NOMENCLATURE (continued)

Greek Symbols

- ρ fluid density
 η condensation efficiency (Equation 9)
 λ property term in thermodynamic ratio (Equation 5)
 σ surface tension

Subscripts

- g gas
f liquid

PREFACE

This is a Quarterly Progress Report on the Creare Downcomer Effects Program. The general context of this work is a postulated Loss-of-Coolant Accident (LOCA) in a Pressurized Water Reactor (PWR), although many of the basic processes being studied may also apply to Boiling Water Reactors (BWRs). The program is a continuing effort to develop analytical and empirical tools which will contribute to best-estimate and licensing predictions of lower plenum filling during postulated LOCAs in PWRs and to assist in the design and specification of larger scale plenum filling tests and the predictions of those test results.

The Creare Downcomer Effects Program is a separate-effects model study of the two-phase flow behavior in the downcomer and adjacent regions of a PWR during the latter stages of blowdown and during refill of the lower plenum in the event of a LOCA. Recognizing the complexity of the underlying phenomena and the limitations imposed by the state of the art of two-phase flow analysis, a balanced program of research experiments and semi-empirical analysis is being pursued. Efforts are divided into 11 interrelated topics:

- A. Model Synthesis
- B. Ramped Transients
- C. Condensation-Induced Transients
- D. Countercurrent Flow
- E. Extended Superheated Walls
- F. Lower Plenum Voiding
- G. Boundary Conditions and Internal Idealizations
- H. Refill Modeling in RELAP
- I. System Effects
- J. Technical Assistance and Review Group Participation
- K. Downcomer Flow Topography Instrumentation

This is a Progress Report on the topic of countercurrent flow.

1 INTRODUCTION

1.1 General Background

During the later stages of blowdown of a Pressurized Water Reactor (PWR) following a hypothesized Loss of Coolant Accident (LOCA), steam generated by heat transfer and flashing flows up the annular downcomer between the core barrel and the pressure vessel on its way to the break (Figure 1). At the same time, Emergency Core Coolant which is being injected into the cold legs attempts, under gravity, to flow through the downcomer to the lower plenum region. The purpose is to refill the lower plenum with water, initiate reflooding of the core, and ultimately cool the core and maintain it in a coolable geometry.

During the refill period, from the start of ECC injection to the beginning of core reflood, a number of processes may interact to impede refill of the lower plenum. Block [1] provides an overview of this behavior. Briefly, flow of steam up the annulus and out the break exerts a drag force on the ECC and may drive it out the break, a process termed ECC bypass.

There are several sources of steam flow in the downcomer. Steam flows directly to the plenum from the core (produced by flashing and heat transfer throughout the system) and is particularly produced by flashing of fluid accumulated in the lower plenum. In addition, steam everywhere in the system may flow through the cold legs and into the downcomer; this steam may assist ECC bypass directly by exerting a force on the water or indirectly by heating it. A key source of steam is boiling of the ECC itself by heat transfer from the superheated metal walls of the lower plenum and annulus.

Since the ECC is highly subcooled, condensation can also occur. Condensation removes steam locally, causing a flow of steam to regions where cold liquid is introduced. This affects the blowdown both by decreasing the flow rate of steam out the break and by altering the split of steam among the various flow paths. Condensation in the lower plenum and annulus tends to suppress ECC bypass by reducing the local steam velocities and hence the steam flow out the break. Condensation can also drive flow and pressure oscillations throughout the system and cause local pressure spikes when steam cavities collapse or slugs of liquid impact structures.

Finally, fluid delivered to the lower plenum may be voided by flashing and heat transfer there and by steam flow into the lower plenum from the core. This voiding tends to delay refill and may also affect the flow behavior in the annulus.

1.2 Countercurrent Flow Studies

A number of experimental studies of the refill period have treated idealized situations where individual processes and sources of steam could be isolated for independent study. Figure 2 shows the situation considered in this report, which is referred to as a countercurrent flow experiment. Steam is supplied by a boiler at a fixed mass flow rate to the core of a scale-model reactor vessel. The vessel walls are initially at saturation temperature. At time zero, ECC is suddenly supplied at a fixed rate and temperature to the model cold legs. There is no steam flow in the cold legs. The pressure in a simulated "containment" at the exit of the model broken leg is maintained at a nearly constant value during each test. Test parameters include the containment pressure, steam flow rate, ECC flow rate, ECC temperature and the vessel geometry. The timing and volume of ECC delivered to the lower plenum is recorded as a function of time. (A number of other pressure, temperature and local flow topography variables may also be recorded in some facilities.) A large quantity of such data has been obtained in the past five years. The particular facility used at Creare is described in Reference [30].

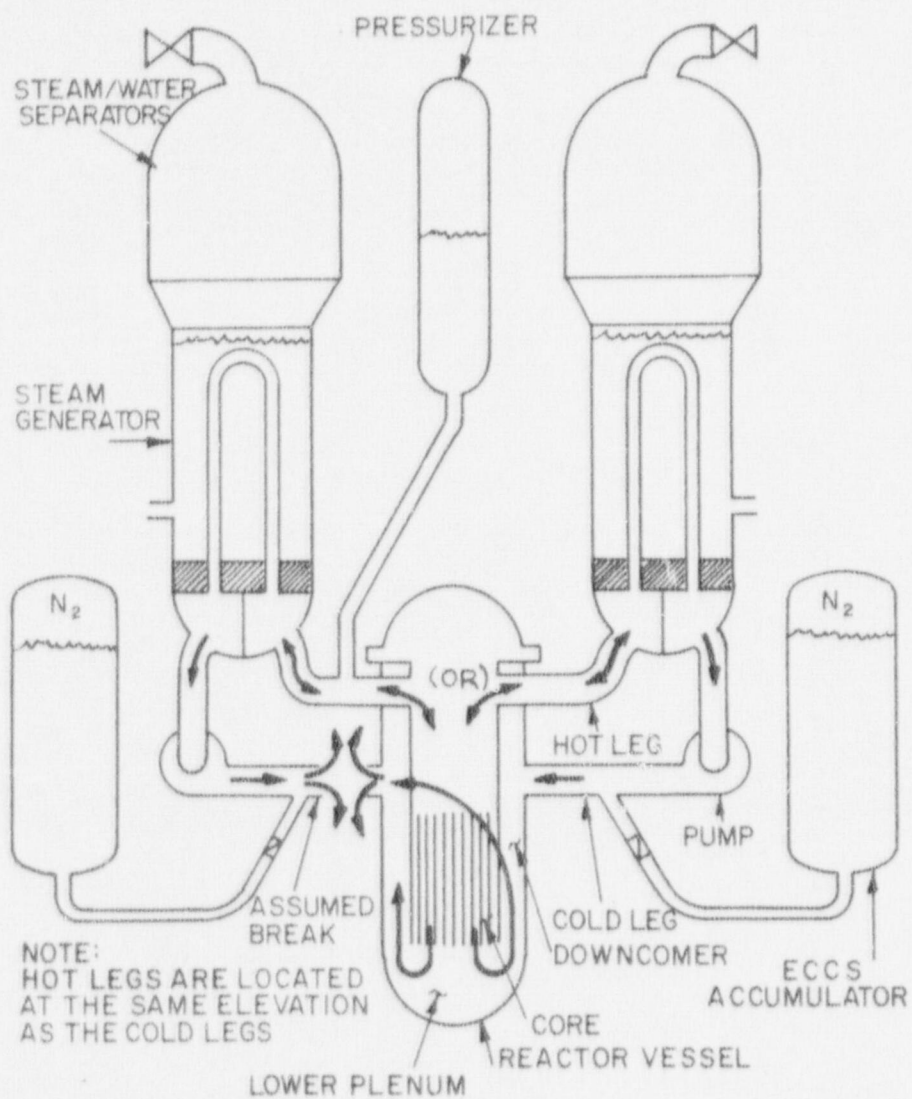


Figure 1. POTENTIAL FLOW PATHS FOR A COLD LEG BREAK IN A PWR

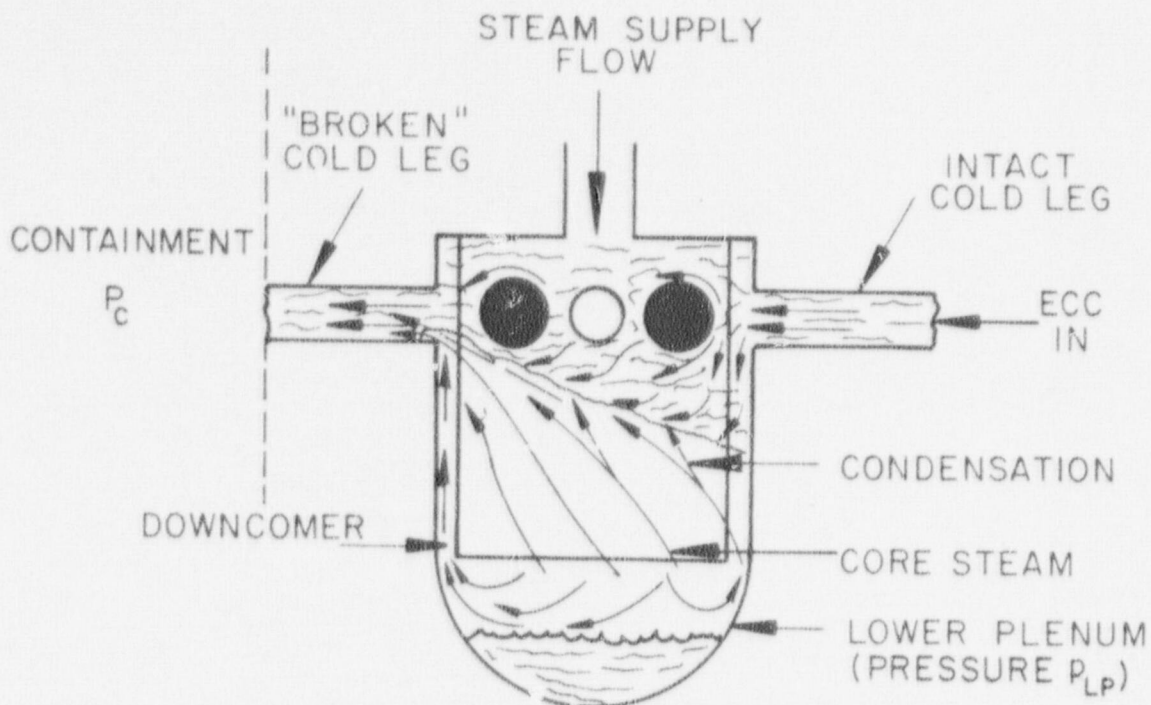


Figure 2. IDEALIZED COUNTERCURRENT FLOW SITUATION

Since it has not yet been possible to derive a reliable analysis of countercurrent flow behavior from first principles, work to date has been largely empirical. Considerable effort has been invested in developing correlations of the data. Such correlations serve two goals. First, they are a shorthand representation of the data. Armed with some equations and some knowledge of the range of parameters tested, one is able to quickly generate a reasonable approximation of the data base. Statistical data analysis on a computer is well suited to meeting this goal. A second goal is to unify and distill the data to extract some understanding of the countercurrent flow behavior. Such understanding may allow us to extrapolate the data base to predict the behavior at physical scales, flow rates, and pressures beyond those tested. (Although future tests may prove such predictions unreliable, they at least provide a basis for the design of a relatively few critical verification tests.) This second goal is more elusive. It requires subjective methods of data analysis and lacks a clear success criterion. We address both goals in this report.

1.3 Summary of This Report

This report presents our correlations of countercurrent flow data and discusses the status and applications of such correlations. Relevant literature is reviewed and comparisons are made with data and correlations developed by other groups.

We focus on the effects of pressure and subcooling and we report our new findings:

- 1) Data obtained for the first time with nearly saturated water at pressures in the range 15 to 65 psia overlay when plotted on J^* coordinates (or any other dimensionless coordinates based similarly on steam momentum flux).
- 2) New data are presented with pressure and subcooling varied independently over much larger ranges than have been studied heretofore.
- 3) It is possible to fit saturated water data with a single functional relation in J^* coordinates that is insensitive to vessel pressure or ECC injection rate.
- 4) It is possible to fit the entire data matrix for subcooled water by a correlating concept that relies on thermodynamic ratio R_T rather than vessel pressure or ECC subcooling independently.

Based on the above findings a relatively simple data correlation concept is proposed.

Previous analysis of earlier data has suggested that ECC subcooling might help to suppress ECC bypass significantly. However, we now project that at pressures typical of calculated reactor conditions during hypothetical LOCA transients there may be little difference between the countercurrent flow behavior of saturated water and the behavior of subcooled water (assuming that the steam flow rate is given). Moreover, reliable methods of scaling condensation rates or the effects of condensation on ECC bypass have not yet been devised. Therefore, in bounding calculations of refill following a postulated LOCA, it would be prudent to take no credit for the possible benefits of ECC subcooling with respect to ECC bypass. However, the effects of ECC subcooling should be included in the calculation of annulus steam flow rates with appropriate allowances to account for uncertainties in modeling condensation.

This report is organized as follows. After a brief review of the literature, our recent data are presented in the context of our new correlation concepts. Subsequently, we examine the scaling of countercurrent flow. Finally, we list conclusions and identify needs for further work. Data tables are provided in Appendices to this report.

2 CONTEXT OF PREVIOUS RESEARCH

An extended literature review is provided as Appendix A of this report and is subdivided into two parts reviewing studies of geometric parameters and thermal/hydraulic parameters respectively. Each part is summarized in turn below.

Correlation of Geometric Parameters

Briefly, we find that although a large number of geometric parameters have been studied extensively, few of these tests have had an impact on data correlations. We have found that annulus gap is not an appropriate dimension to use as a characteristic length scale in dimensionless ECC bypass parameters. Instead, Creare proposed the use of J^* parameters based on annulus circumference w unless and until additional data suggesting a different dimension become available. We also find that although J^* scaling represents available data from small scale models, reliable methods to extrapolate to PWR scale have not yet been devised.

We have learned that the filling behavior is relatively insensitive to lower plenum depth and broken leg diameter if all other parameters (e.g., vessel pressure) are fixed. However, a deep lower plenum is helpful to get accurate plenum filling data and a large broken leg enhances vessel pressure control. Certain geometric details such as intact cold leg diameter, annulus length, hot leg plugs, and cold leg arrangements have little or no effect on plenum filling. However, some other geometric details such as annulus baffles or distributed obstructions such as pins have had appreciable effects on the rate of plenum filling.

Correlations in use reflect the geometry mainly through the choice of a single dimension for insertion in dimensionless parameters such as J^* . Factors have not yet been developed to account for other known geometric effects.

Correlation of Thermal/Hydraulic Parameters

Thermal/hydraulic parameters that have been systematically varied have included steam supply rate, ECC injection rate, vessel pressure, and ECC subcooling.

Figure 3 shows idealized data forming a penetration curve on a map of dimensionless core steam flow J_{gc}^* and dimensionless delivery rate J_{fd}^* where:

$$J_{gc}^* = \frac{\rho_g^{1/2} j_g}{[gw(\rho_f - \rho_g)]^{1/2}} \quad (1)$$

$$J_{fd}^* = \frac{\rho_f^{1/2} j_f}{[gw(\rho_f - \rho_g)]^{1/2}} \quad (2)$$

In this formulation the j 's are defined as superficial velocities of each phase calculated as if that phase were flowing alone and uniformly filled the annulus cross-section. (Note that in the mapping of Figure 3 the ordinate is the independent test variable following the usual convention for countercurrent flow studies.)

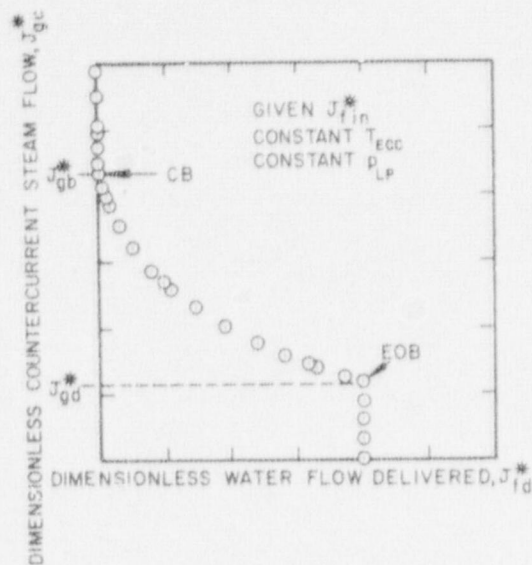


Figure 3. IDEALIZED ECC BYPASS DATA

We define two critical steam fluxes, the complete bypass point J_{gb}^* and the complete delivery point J_{fd}^* so that the data include three idealized ranges of behavior:

- 1) all the ECC is bypassed in the range $J_{gc}^* > J_{gb}^*$,
- 2) there is partial ECC delivery in the range $J_{gd}^* < J_{gc}^* < J_{gb}^*$,
- 3) all the ECC is delivered in the range $0 < J_{gc}^* < J_{fd}^*$

It should be pointed out that actual data may deviate slightly from this idealization. Even at high steam flux $J_{gc}^* > J_{gb}^*$ a tiny occasional splash of water may be delivered. Also the delivery rate at complete delivery can be several percent higher than the ECC injection rate when condensate is included.

Efforts have focused on correlation of the partial delivery range and thereby on its limits of the complete bypass point (designated CB on Figure 3) and the complete delivery point (also known as the end of bypass point and designated EOB on Figure 3).

Attempts have been made to represent the effects of the three key parameters, namely, ECC injection rate, ECC subcooling, and vessel pressure on the penetration curve. However, repeated iteration between testing and analysis has been required because the parameters have coupled effects and because it is difficult to control the parameters entirely independently. (For example, increased injection rate tends to increase the broken leg pressure drop. This in turn increases vessel pressure at fixed containment pressure and thereby increases ECC subcooling at fixed ECC temperature.)

Early reports prepared by Dartmouth, Battelle, and Creare [2,3,4,5] describe various approaches to correlating data. Three prime concepts emerge:

- 1) countercurrent flow behavior in small scale models with saturated water can be represented by dimensionless J^* parameters,
- 2) the additional effects of condensation can be accounted by reducing the supplied core steam flow by an "effective" condensed flow, and
- 3) the effective condensed steam flow is related to the amount that could be condensed ideally in raising the injected ECC to saturation temperature at thermodynamic equilibrium.

The history of efforts to correlate countercurrent flow data is outlined in Appendix A. Briefly, Battelle has proposed eight specific correlation forms over the past four years and has gradually refined the choices of correlation coefficients [3,6,7,8,9,10,11,12]. Creare proposed a countercurrent flow correlation in 1976 [13] and demonstrated its application to the "hot-walls" analysis derived originally in 1974 [14]. In this report we describe several new correlating concepts that take advantage of recent experimental findings on the effects of pressure and subcooling. These concepts are implemented by modifying coefficients in our 1976 correlation. It is gratifying that these refinements simplify the correlation and permit us to reduce or eliminate deviations from the prime concepts listed above.

3 CORRELATION OF PRESSURE AND SUBCOOLING EFFECTS

Here we report recent gains in understanding and correlating saturated water behavior and the additional interrelated effects of pressure and subcooling. We then present our correlation and compare it with available data. New data covering an expanded range of pressure and subcooling are presented and form the basis for upgrading the correlation coefficients.

3.1 The Countercurrent Flow Correlation

The basic equations of our correlation are unchanged from those proposed in 1976 [13]. In present nomenclature, the equations describing the partial delivery range are:

$$J_g^{*h} + mJ_{fd}^{*h} = C \quad (3)$$

$$J_g^* = J_{gc}^* - f\lambda J_{fin}^* \quad (4)$$

where C , m , and f are coefficients to be determined empirically, and:

$$\lambda = \frac{C}{P} \frac{(T_s - T_{ECC})}{h_{fg}} \sqrt{\frac{\rho_f}{\nu_g}} \quad (5)$$

In fitting the data and in using the correlation we follow a systematic approach motivated by our view of the physics:

- 1) the coefficient C is given by J_{gb}^{*h} where J_{gb}^* is the complete bypass point for saturated water,
- 2) the condensation coefficient f is determined from the complete bypass points for water with various subcoolings, and
- 3) the slope coefficient m is determined from the entire data base with C and f fixed.

This approach reflects our view that the complete bypass points are relatively stable operating points that can be repeated by different investigators. It is our observation [15,16] that the partial delivery range is dynamically unstable, often producing slug flow with subcooled water. Although an adequate analysis of the slug delivery instability has not yet been developed, it has been shown experimentally that such factors as compliance of the steam supply, lower plenum vapor volume, and containment compliance or air content can strongly affect the flow stability (i.e., the presence or absence of slug delivery). In this situation, the partial delivery range is unlikely to represent the countercurrent flow physics generally, although the data are likely to have systematic trends for any given facility. For this reason we are employing a correlation approach which focuses on the complete bypass points while representing the remaining data more approximately.

Recognizing that there is independent interest in the end-of-bypass point, we also identify an appropriate minimum value of steam flow below which complete delivery always occurs.

In implementing our correlational approach, we have been careful to obtain data that extend into the complete bypass range. By this means we are able to interpolate data near complete bypass and are thus able to avoid unreliable extrapolation from the partial penetration range.

Table 1 compares the functional relations in the previous and present correlation concepts. Relative to Reference [13], the present correlation includes:

- 1) an improved value for C,
- 2) elimination of the pressure effect in f ,
- 3) recognition that the slope m
 - a) is a constant (i.e., m is not a function of injection rate) for saturated water and steam as well as for air and water, and
 - b) is adequately represented by a function of thermodynamic ratio for subcooled water.

Item 1 is the result of earlier Creare work [17] and is also consistent with statistical analysis performed by Battelle [12]. Item 2 has also been identified by Battelle [10] as an outcome of their statistical studies in a different correlation context. Item 3 is suggested here for the first time.

In this report we focus our attention on a single ECC injection rate, $J_{fin}^* = 0.116$ in order to emphasize the effects of pressure and subcooling. For this injection rate, $f = 0.16$. The coefficient m is shown graphically in Figure 4.

Coefficient	Previous Correlation [13]	Present Correlation
C	0.32	0.40
f	$f(P_{LP}, J_{fin}^*)$	0.16 (at $J_{fin}^* = 0.116$)
m	$m(J_{fin}^*)$	$m(R_{Tb})$

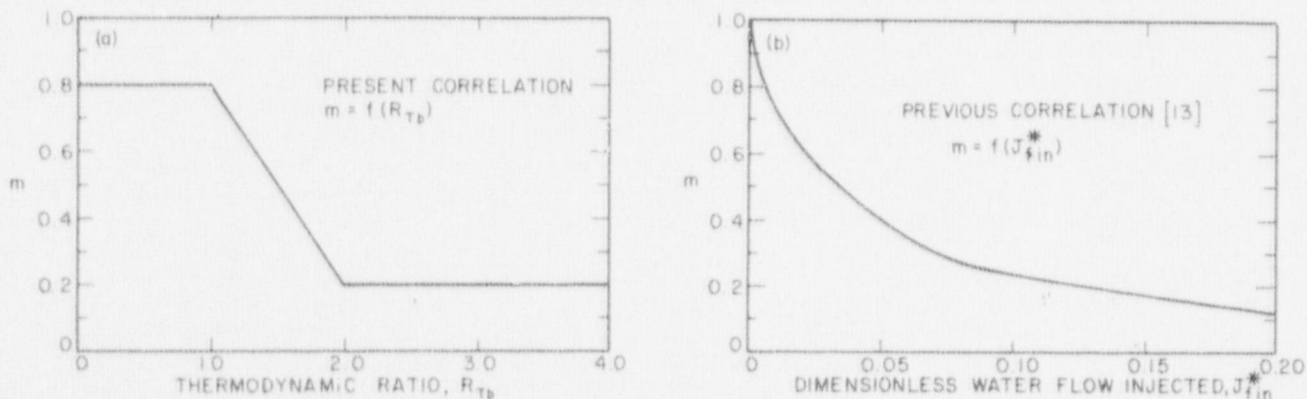


Figure 4. BEHAVIOR OF FACTOR m REPRESENTING PARTIAL DELIVERY

In addition to modifying the coefficients, our present correlation has two additional aspects. First, we calculate complete delivery for all $J_{gc}^* < 0.04$. Although a better description of this deviation from the Wallis correlation is desirable, this simple criterion reasonably represents available data [15,17,18]. Secondly, for the purpose of calculating delivery rates we are using the thermodynamic ratio at the complete bypass point for the particular values of P_{LP} , T_{ECC} , and J_{fin}^* :

$$R_{Tb} = \lambda J_{fin}^* / J_{gb}^* = \frac{c_p (T_s - T_{ECC})}{h_{fg}} \sqrt{\frac{\rho_f}{\rho_g}} \frac{J_{fin}^*}{J_{gb}^*} \quad (6)$$

Thus, to calculate a delivery curve for a given injection rate, pressure, and subcooling, the complete bypass point is first determined from the explicit equation:

$$J_{gb}^* = C^2 + f \lambda J_{fin}^* \quad (7)$$

Then m is evaluated from Figure 4 and with ($f=0.16$) Equations (4) and (3) are solved in order for each value of J_{gc}^* along the curve. From Equations (6) and (7) we find that the complete bypass point can also be stated implicitly in terms of the thermodynamic ratio:

$$J_{gb}^* = \frac{C^2}{1 - f R_{Tb}} \quad (8)$$

The motivation for these changes in our correlation will be discussed further as we compare the correlation with data in the following sections of this report.

3.2 Creare Saturated Water Data

Figure 5 compares our correlation (Equations 2 to 6) with data for ECC temperatures very near to saturation [17]. It can be seen in both the data and the calculated curves that the very low subcoolings in these tests (numbers near some of the data points) have a very weak effect on delivery rate. Injection rate also has little effect in these tests with low subcooling.

Figure 6 compares our correlation for saturated water with data for nearly saturated water at pressures in the range 15 to 65 psia. These data, shown here for the first time, provide an important verification of the basic assumption in all previous correlations that saturated water behavior is insensitive to pressure. That is, countercurrent flow data for various pressures collapse to the same curve when plotted in conventional J^* parameters. By the same measure, J^* parameters properly account for the effects of pressure, at least for saturated water.

The proposed transition to complete delivery at $J_{gc}^* = 0.04$ is shown in Figures 5 and 6 to provide a reasonable lower limit for the data.

In summary, when the injected ECC is at or very near saturation temperature, we have found that neither the injection rate nor the vessel pressure significantly affects delivery as a function of dimensionless steam flux J_{gc}^* . The lack of an injection rate effect has been shown at both 1/30 and 1/15 scale [17]. Further confirmation of these findings with air and water or at other scales and pressures would be desirable.

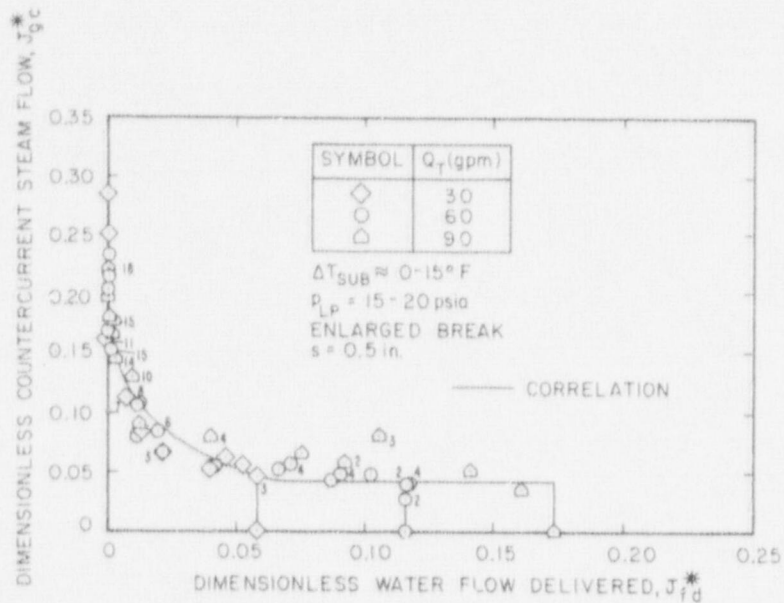


Figure 5. COMPARISON OF PRESENT CORRELATION WITH CREARE 1/15-SCALE DATA FOR SATURATED WATER AT SEVERAL ECC INJECTION RATES [17]

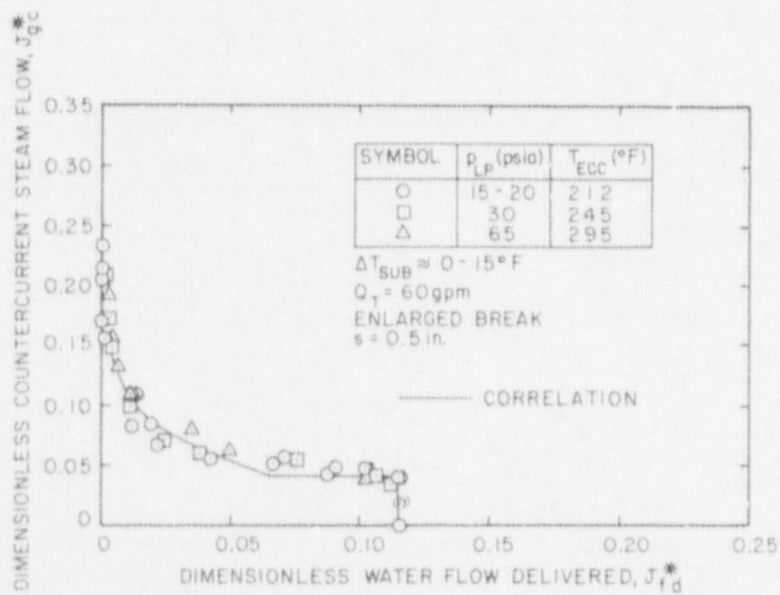


Figure 6. COMPARISON OF PRESENT CORRELATION WITH CREARE 1/15-SCALE DATA FOR SATURATED WATER AT SEVERAL VESSEL PRESSURES

3.3 Creare Data for Effects of Condensation

Figure 7 compares our correlation with data at various subcoolings (ECC temperatures). Vessel pressure is near ambient pressure. The delivery curves shift upward as subcooling is increased as has been observed repeatedly in previous work by Dartmouth, Battelle and Creare. The correlation is a reasonable fit to the data.

Figure 8 also compares our correlation with data for various subcoolings, but at a fixed vessel pressure of 65 psia. Again the delivery curves shift upward as the subcooling is increased. However, comparison of Figures 7 and 8 reveals that at higher pressures a larger subcooling is required to produce a specified upward shift. Inspection of Equation (6) for R_{TP} reveals that gas density appears in the denominator and tends to weaken the effect of subcooling as pressure is increased. The correlation is a reasonable fit to these data shown here for the first time and extending over a 220°F range of subcooling.

Figure 9 compares our correlation with new data at various pressures for a fixed ECC subcooling of 135°F. Although saturated water data are insensitive to pressure, subcooled water data are strongly affected by pressure. As pressure is increased at fixed subcooling, the delivery curves shift downward on J^* coordinates. Even at moderate pressures, the subcooled water curves approach the saturated water curve. The correlation is shown for several additional pressures beyond the data base to emphasize this point. Said differently, subcooling is not very important to ECC delivery except at pressures near atmospheric pressure.

Figure 10 compares the previous Figures 6, 8, and 9 to show that these data are well represented as a function only of R_{TP} . The very rapid downward shift of the data in the range $1 < R_{TP} < 2$ is notable.

All of these data are for a single injection rate. We anticipate that the same correlation concepts will be extended to treat other injection rates.

Figures 7 to 10 demonstrate that the correlation acceptably fits data over a broad range of pressures and subcoolings. Varying either parameter gives a fan of curves with similar appearance: as the curves shift up, their slopes tend to zero. Our correlation has been designed to reflect this trend by having both the complete bypass point and the slope be a function of thermodynamic ratio.

It is satisfying to be able to correlate this broad range of data, and the additional data presented in the following sections, with a constant factor "f", and a simple dependence of both the complete bypass point and the slope on a single dimensionless parameter R_{TP} . Discussion of the physical motivation for this approach and our numerical methods is deferred to Section 3.5 so that we may present comparisons with the remaining data.

3.4 Comparisons With Additional Creare Data

Figure 11 compares the correlation with a set of data for 212°F ECC with a "scaled" (1.875 inch diameter) broken leg. These data may be compared with those of Figure 5 which are also for 212°F ECC but with an oversize (3.0 inch diameter) broken leg. The oversized broken leg keeps the pressure close to ambient pressure and thus the subcooling close to zero. In Figure 11 it can be seen that the subcoolings (numbers near data points) increase as complete bypass is approached. (As more water is bypassed the broken leg pressure difference and hence the vessel pressure increase.) The correlation correctly reflects this effect.* Thus, the break size affects ECC bypass through its effect on pressure or subcooling and this effect is accounted by the present correlation.

*In order to draw these correlation lines we have fit the curves using the measured pressures corresponding with the data.

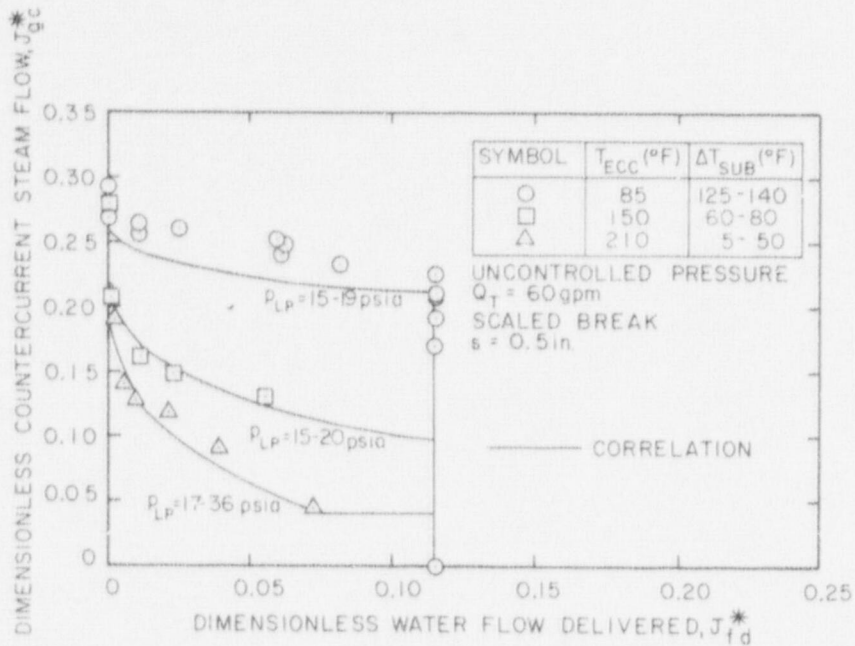


Figure 7. COMPARISON OF PRESENT CORRELATION WITH CREARE 1/15-SCALE DATA FOR SUBCOOLED WATER NEAR AMBIENT PRESSURE [16]

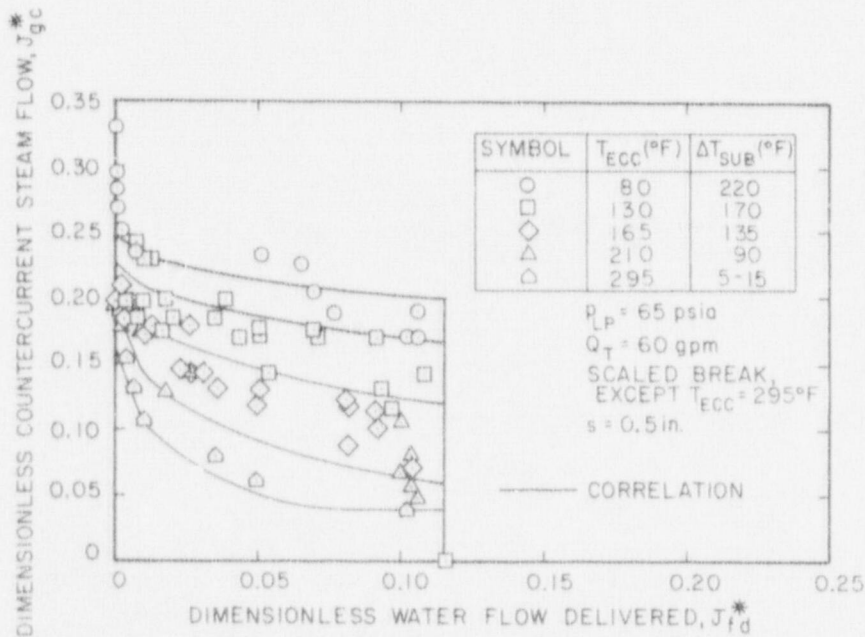


Figure 8. COMPARISON OF PRESENT CORRELATION WITH CREARE 1/15-SCALE DATA FOR A VESSEL PRESSURE OF 65 PSIA AT VARIOUS ECC SUBCOOLINGS

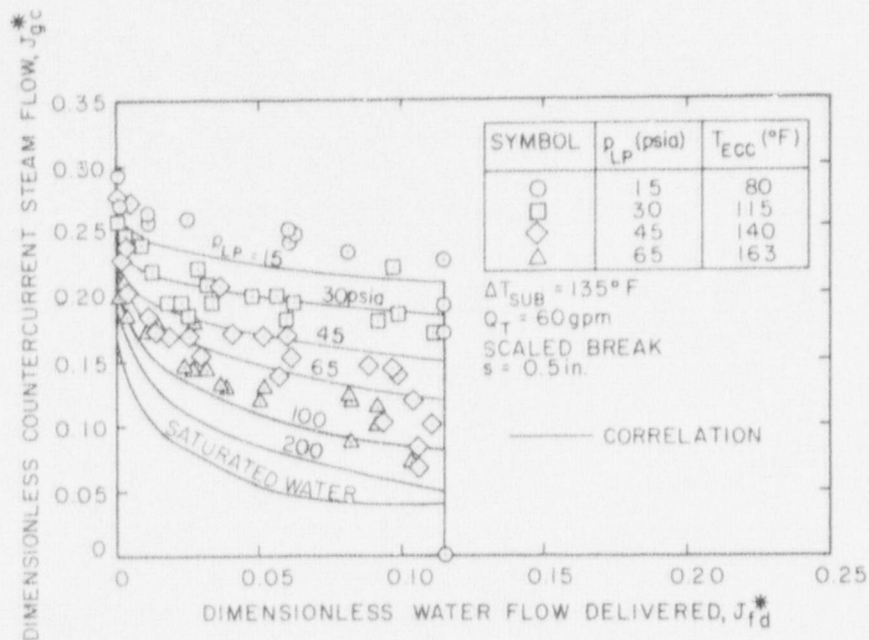


Figure 9. COMPARISON OF PRESENT CORRELATION WITH CREARE 1/16-SCALE DATA FOR AN ECC SUBCOOLING OF 135°F AT SEVERAL PRESSURES

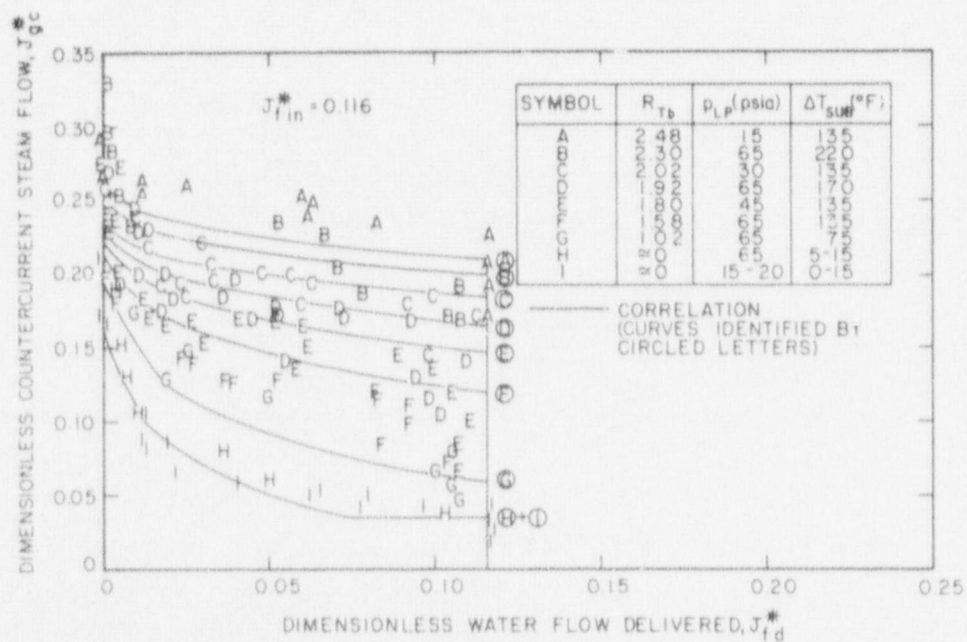


Figure 10. COMPARISON OF PRESENT CORRELATION WITH PRESENT CREARE DATA FOR VARIOUS PRESSURES AND SUBCOOLINGS ARRAYED AS A FUNCTION OF THERMODYNAMIC RATIO

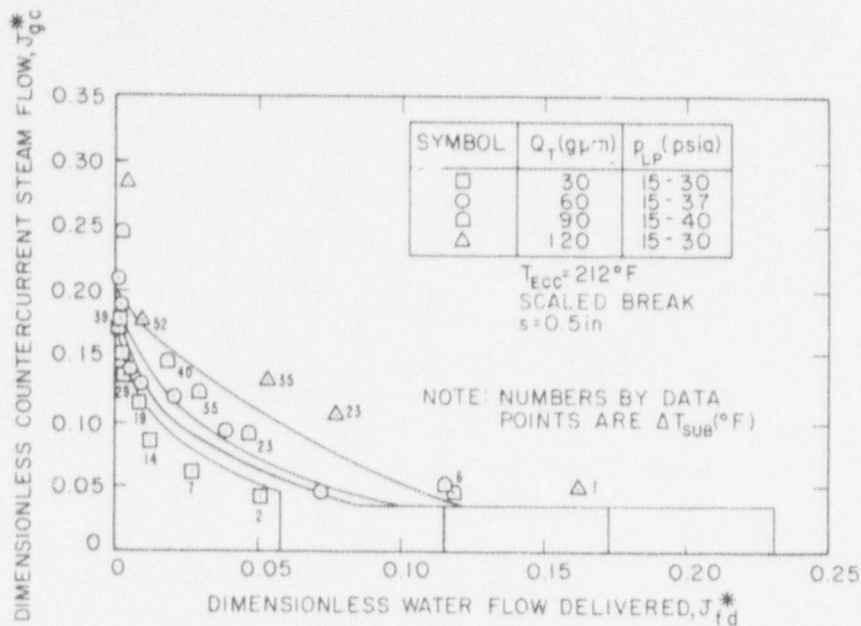


Figure 11. COMPARISON OF PRESENT CORRELATION WITH EARLIER CREARE 1/15-SCALE DATA FOR 212°F ECC AT SEVERAL INJECTION RATES AND UNCONTROLLED PRESSURES

The data of Figure 11 also display an apparent effect of ECC injection rate. However, comparison with Figure 5 shows that this too is an effect of condensation due to subcooling. In addition to Figure 5, Figures 25 and 26 of Reference [16] reveal that a factor of 250 change in ECC momentum (effected by varying the intact cold leg diameter) had a negligible effect on delivery. In earlier work, the trend with injection rate in Figure 11 was erroneously believed to be a real effect of ECC momentum with saturated water and was reflected in our 1976 correlation by the function $m(J_{fin}^*)$ shown in Figure 4. (This same function was later adopted by Battelle and they are currently using a similar function [12].) We are now able to remove this incorrect dependence on J_{fin}^* .

Believing that there is more to be learned about the proper scaling of the effects of injection rate on condensation (with subcooled water), we are not yet presenting a correlation of this parameter. It is possible, though we will try to avoid it, that either f or m will have to be refined for it to include J_{fin}^* independently. In a later report we will present a refined correlation approach and compare it with additional data at various injection rates.

The test matrix for the new data presented in this report, all at $J_{fin}^* = 0.116$, is shown in Table 2. Comparisons of our correlations with these data are shown in Figures 12 to 15 (together with the earlier Figures 6 to 9). As might be expected, the correlation is successful at intermediate pressures and subcoolings as it was at the limiting values shown in Figures 6 to 9. These data are tabulated in Appendix B.

TABLE 2							
MATRIX OF RECENT CREARE TESTS*							
Pressure (psia)	Subcooling (°F)						
	=0	65	90	135	170	195	220
Ambient	X	0		X			
30	X			0	0		
45		0		0		0	
65	X		0	0	0		0

All tests are for $J_{fin}^ = 0.116$. Some tests were performed with an oversized broken leg (X), and others with a scaled broken leg (0).

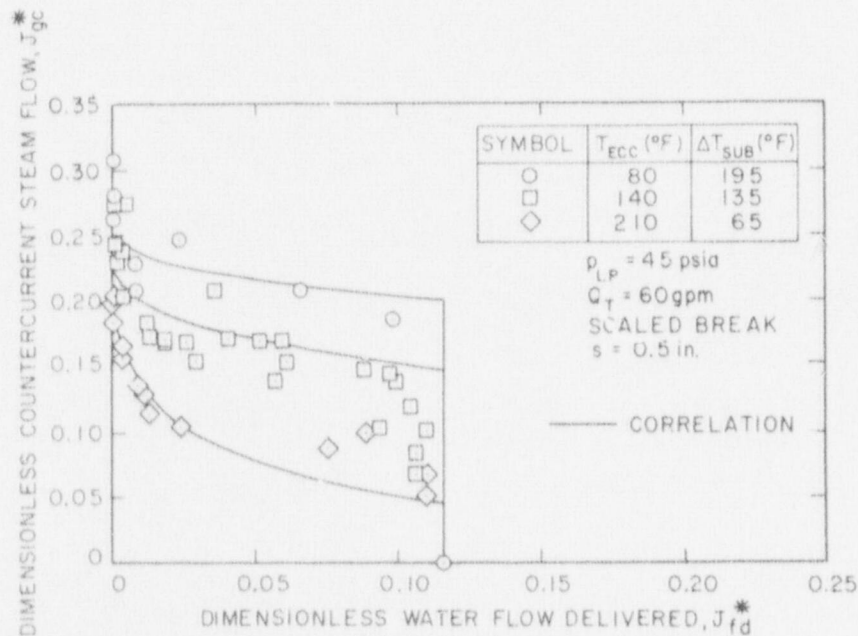


Figure 12. COMPARISON OF PRESENT CORRELATION WITH CREARE 1/15-SCALE DATA FOR 45 PSIA VESSEL PRESSURE AT VARIOUS ECC SUBCOOLINGS

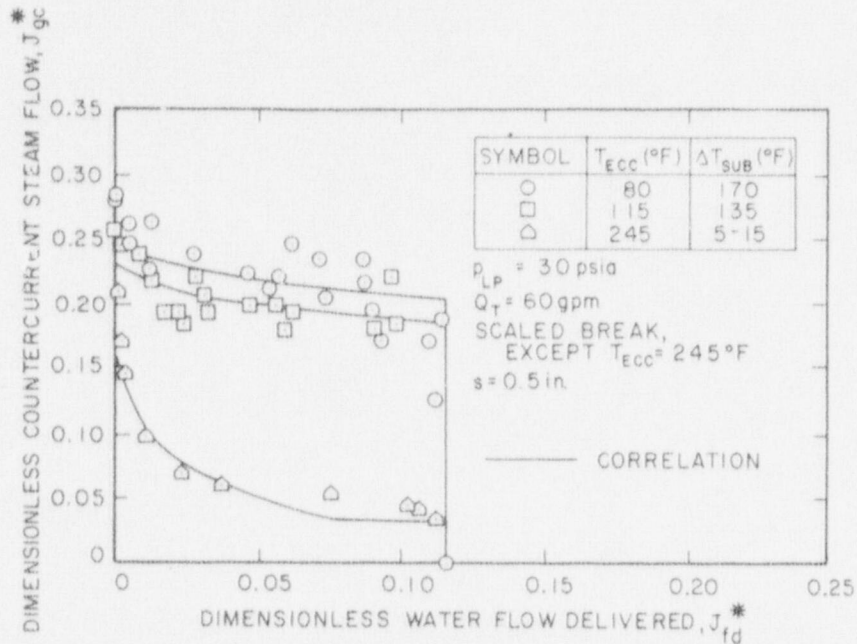


Figure 13. COMPARISON OF PRESENT CORRELATION WITH CREARE 1/15-SCALE DATA FOR 30 PSIA VESSEL PRESSURE AT VARIOUS ECC SUBCOOLINGS

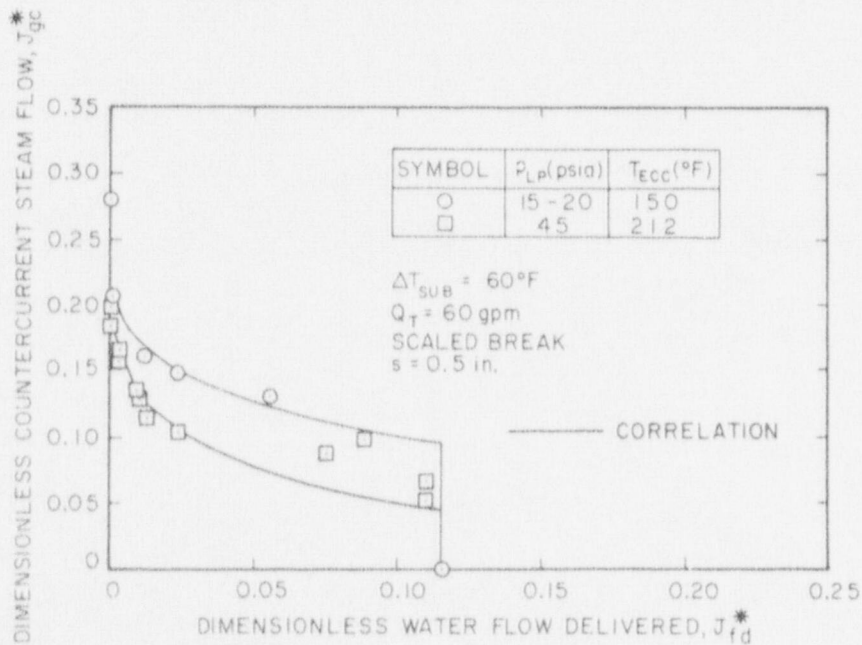


Figure 14. COMPARISON OF PRESENT CORRELATION WITH CREARE 1/15-SCALE DATA FOR 60°F ECC SUBCOOLING AT VARIOUS PRESSURES

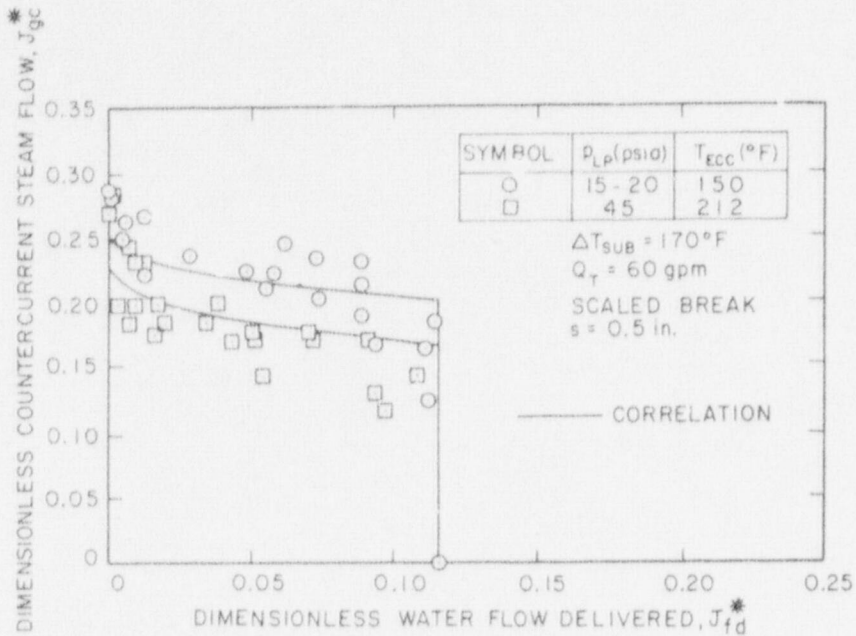


Figure 15. COMPARISON OF PRESENT CORRELATION WITH CREARE 1/15-SCALE DATA FOR 170°F ECC SUBCOOLING AT VARIOUS PRESSURES

Table 3 displays the test matrix for previously reported countercurrent flow tests in this facility [16,17]. (These tests were generally performed near ambient pressure and typical data are displayed in Figures 7 and 11.) In addition, some very early (1975) tests were performed in a crude temporary vessel mainly to assist facility design [18,30]. Although these latter tests provided the first data for pressures significantly above ambient, they have been superseded.

TABLE 3						
<u>CREARE DATA REPORTED PREVIOUSLY*</u>						
ECC Subcooling (°F)						
J_{fin}^*	0	60	110	135	170	210
0.02				X		
0.03	○	○				
0.06	X ○ Δ	X ○	X	X ○ Δ		
0.12	X ○ Δ	X ○	X	X ○ Δ		
0.18	X ○ Δ	X ○	X	X ○		
0.23	X Δ	X	X	X Δ		

*All tests performed with vessel near ambient pressure.

X - Small Gap, Scaled Break [16]
 ○ - Large Gap, Scaled Break [16]
 Δ - Small Gap, Oversized Preak [17]

3.5 Correlation Methods

In deriving our correlation, our primary tool has been numerical data fitting to minimize deviation in the least squares sense. We have strived to restrict the parameter dependence of our functions where we could and specifically have assessed the data using a "building block" approach. That is, we have sequentially determined the coefficients C, f, and m by examination of the saturated water complete bypass point, the subcooled water complete bypass points, and the partial penetration range of the data respectively. An alternative approach is to simply use all of the data to determine "best fit" values of C, f, and m. We have done this too, and find that both methods give similar numbers. Since the objective of this progress report is primarily to illustrate the data trends for a subset of the data, we simply chose the coefficients given by the first approach.

The proof of any correlation lies in its ability to represent the data. As part of this proof, we systematically compared the correlation with our data in preceding sections of this report. In the remainder of this section we discuss our rationale for the correlating functions and we display the sensitivity to the correlating parameters.

We should comment that the correlation process is not one that can yet be carried out with scientific rigor. The problem is twofold. First, although the computer will produce coefficients on demand, it is slave to the correlating functions supplied by the user. Secondly, in this field the data are more of a broad survey than they are a statistically significant, properly weighted sample for each parameter effect. Furthermore, a larger fraction of the data (near complete bypass and complete delivery) contain valuable information but are difficult to use in a purely numerical approach because they are near a physical discontinuity. Therefore, we are skeptical of all data analysis in this field and we lack confidence in the results of a purely numerical data analysis. Standard methods of statistical data analysis can place the situation in proper perspective, however, if they weight the data and account for experimental uncertainties.

Correlation Concepts and Physical Rationale

As stated, our correlation has been built by sequentially examining data for:

- 1) the saturated water complete bypass point,
- 2) the subcooled water complete bypass points, and
- 3) the partial delivery range of data.

We have shown that the coefficient C is a constant [17], about 0.4, independent of pressure, injection rate, or scale in the ranges tested. This coefficient C represents incipient countercurrent flow of saturated water. It should be possible to compare this coefficient with values from similar data for air-water and steam-water behavior in a variety of geometries, including tubes, as long as physical effects such as injection method have been properly modeled and methods for accounting significant geometric differences are devised.

The coefficient f has been defined to represent the effects of condensation on the complete bypass point. If condensation proceeded to equilibrium, and if the condensed steam did not contribute to bypass, then f would be unity. In fact, for a scaled injection rate of $J_{fin}^* = 0.116$, we have found that $f = 0.16$, a number well below unity. Therefore, either condensation does not proceed to equilibrium (the water is not heated

to saturation) or some of the steam which is condensed contributes to bypass. Probably, both are true. Typical data for broken-leg water temperature T_{fb} are shown in Figure 16. (The values of T_{fb} were determined from thermocouples and these were checked against water samples drawn from the break.) The data are shown as temperature T_{fb} and also in terms of condensation efficiency defined as

$$\eta_g = R_T \eta_f = R_T \left[\frac{T_{fb} - T_{ECC}}{T_s - T_{ECC}} \right] \quad (9)$$

where R_T is the supply-based thermodynamic ratio given by:

$$R_T = \lambda J_{fin}^* / J_{gc}^* \quad (10)$$

At a subcooling of 130°F, η_g is unity; virtually all the steam is condensed in the vessel. Yet there is also complete bypass. Therefore, some of the condensed steam contributes to bypass. On the other hand, condensation does not always proceed to equilibrium since even η_g is well below unity at subcoolings lower than 130°F and η_f is well below unity for all tests. Said differently, it is certainly unnecessary to raise the water to saturation temperature in order to bypass the water.

Thus, the coefficient f can be seen as a simple factor which reflects both the efficiency of condensation and the effectiveness of the condensed steam in contributing to bypass. These two effects cannot be isolated by study of bypass data alone. However, both effects are related to condensation and tend to zero as condensation is suppressed. It is encouraging that the formulation for complete bypass point (Equation 8) accounts reasonably for the effects of both pressure and subcooling, via R_{TB} , so that the factor f need only be a constant (at least at the one injection rate studied). Although this "f factor" modeling approach is simple, it is consistent with the state-of-the-art as described for example by Jones and Saha [19] and Wallis et. al. [29].

The coefficient m represents the slope of the delivery curve. Figures 8 and 9 show that the slope tends to zero as ECC subcooling is increased or as vessel pressure is decreased. However, Figure 6 shows that the slope is insensitive to pressure for saturated water (zero subcooling). These data are all combined on Figure 10 where thermodynamic ratio R_{TB} is the sole parameter. This figure indicates that the slope is also reasonably expressed as a function only of R_{TB} .

Why does the slope vary in this manner? We can only speculate. Physically, cold water is being delivered to the lower plenum in the partial delivery range of the data. Therefore, there may be condensation in the lower plenum. Any core steam condensed in the lower plenum in these tests makes no contribution to annulus bypass. In contrast, we demonstrated above that steam condensed in the annulus does contribute to bypass. Qualitatively, then, lower plenum condensation tends to be more effective than annulus condensation in suppressing bypass. Since there is more lower plenum condensation with delivery than without delivery, the complete delivery point should shift up more than the complete bypass point as R_{TB} is increased. Thus, the slope of the delivery curve tends to zero as R_{TB} is increased. We hasten to emphasize that this is a purely subjective description of the physics and lacks direct evidence. However, it is a reasonable rationale for expressing the slope coefficient as a function of R_{TB} .

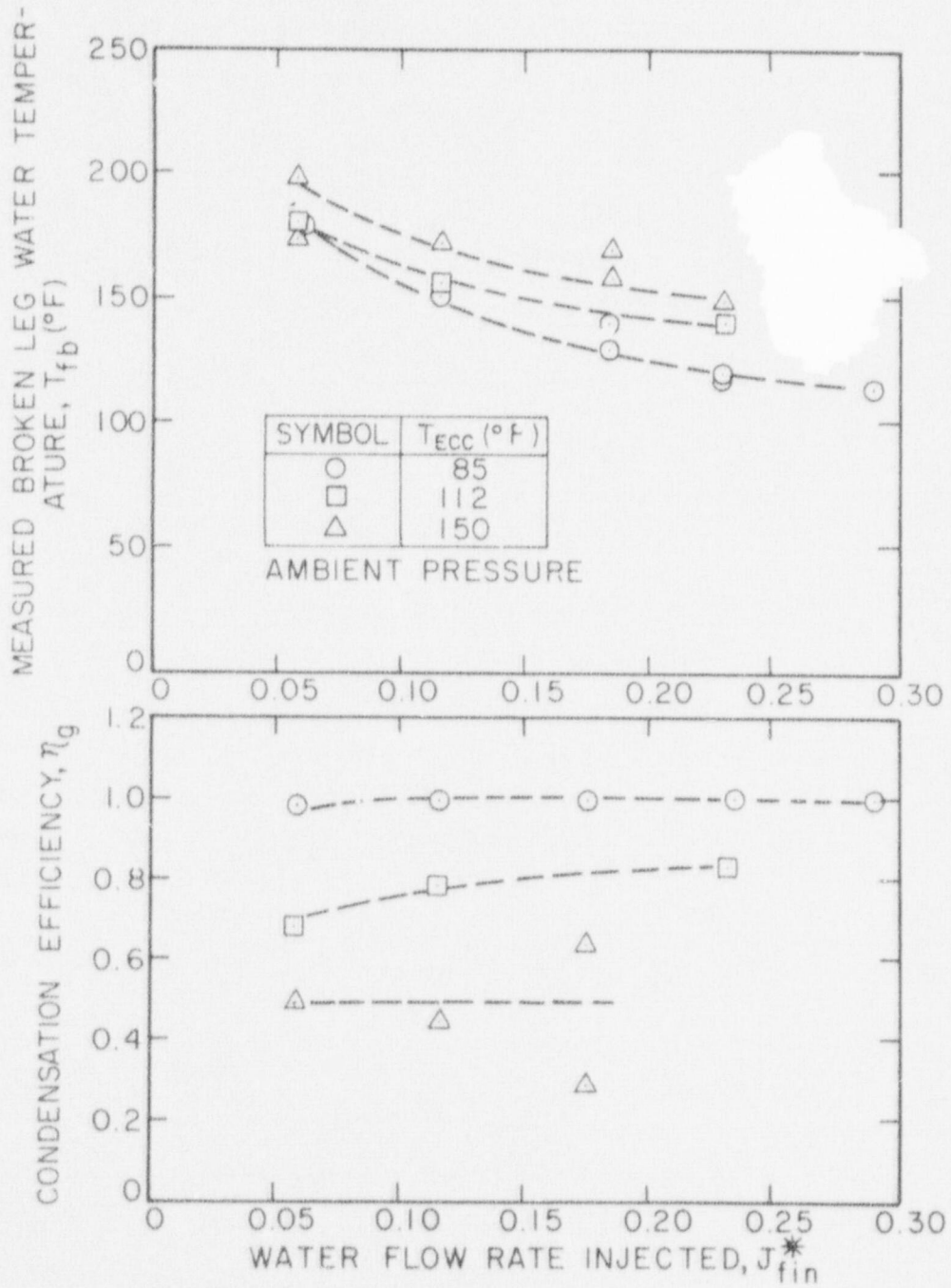


Figure 16. LIQUID TEMPERATURES IN THE BROKEN LEG OF THE CREARE 1/15-SCALE VESSEL DURING COMPLETE BYPASS

The particular function $m(R_{TP})$ shown in Figure 4 was chosen simply as a reasonable fit to the data. Future data may reveal needed refinements. This function derives some basis from earlier work [2,20] where a limiting thermodynamic ratio of unity or the range 1 to 2 has had special importance.

Sensitivity Analysis of Correlation

Figures 17 to 19 compare key data with the 1976 correlation which has coefficients:

$$c = 0.32$$

$$f = \left[\frac{P_{LP}}{P_a} \right]^b \left[\frac{1}{1 + 30 J_{fin}^*} \right]$$

$$m = \exp[-5.6 J_{fin}^{*0.6}] \tag{11}$$

Figure 17 shows that the complete bypass limit c^2 is somewhat too low for saturated water and also that the variable slope $m(J_{fin}^*)$ is inappropriate.

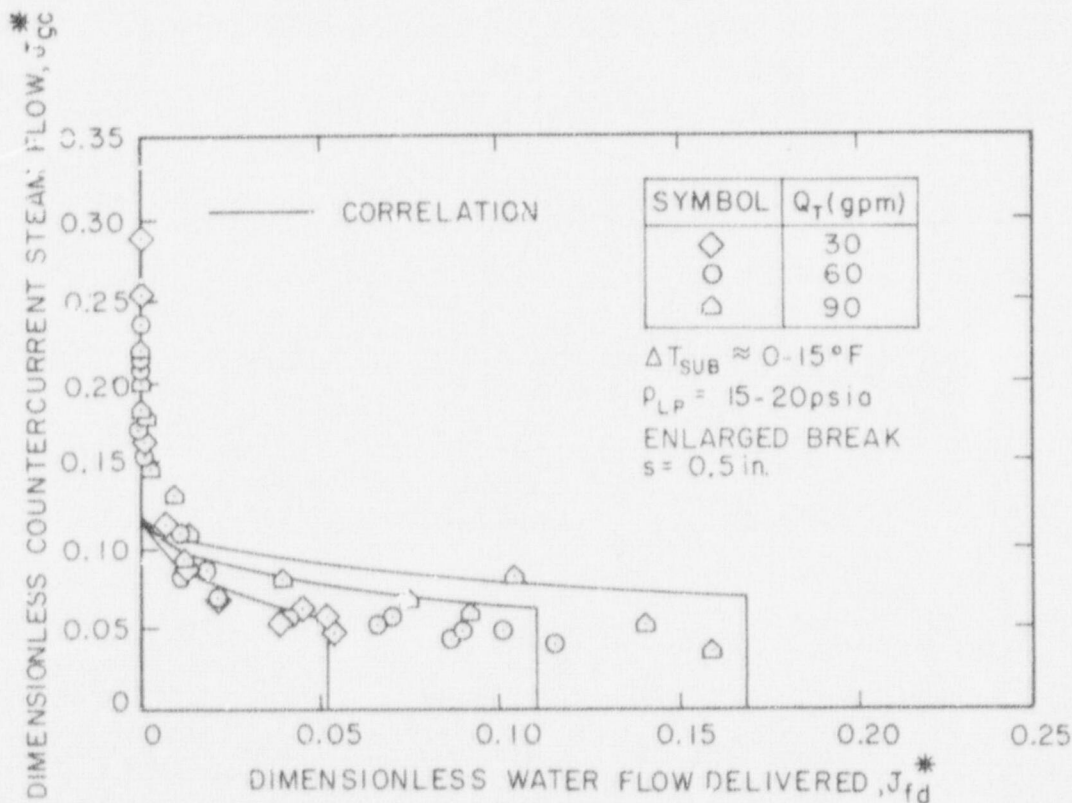


Figure 17. COMPARISON OF PREVIOUS CORRELATION [13] WITH CREARE 1/15-SCALE DATA FOR SATURATED WATER [17]

For subcooled water, Figure 18 shows that the previous correlation [13] represents data at various pressures poorly. (Although it is an adequate fit to the effects of ECC subcooling at ambient pressure, Figure 19, it is unsatisfactory at all other pressures.) The term containing pressure to the quarter power in the factor f in earlier Creare and Battelle correlations [8,13] is simply incorrect. The variation of slope seen in Figures 18 and 19 is also not well represented by the constant value $m=0.21$ for $J_{fin}^*=0.116$. Thus, the superiority of the present correlation has been demonstrated by comparison with earlier ideas.

The sensitivity of the correlation to the coefficients C , m , and f has also been examined. The values of $C=0.4$ and $m=0.8$ (for $R_{Tb}<1$) in our correlation were chosen based upon the countercurrent flow data with saturated water. Figure 20 illustrates that when C is 0.35, the best fit slope to these data is $m=0.4$, and the complete bypass intercept is clearly underpredicted. The figure also shows that when $C=0.45$, the best-fit slope is $m=1.0$ and data near the complete bypass point are slightly overpredicted. In the latter case, data near complete delivery are underpredicted, though the overall fit is qualitatively similar to $C=0.4$ and $m=0.8$ (see Figure 6). Thus, the data are more obviously sensitive to lower rather than higher values for C and m , given the same perturbation of C in either direction. Higher values of C than 0.45 would become unreasonable, however.

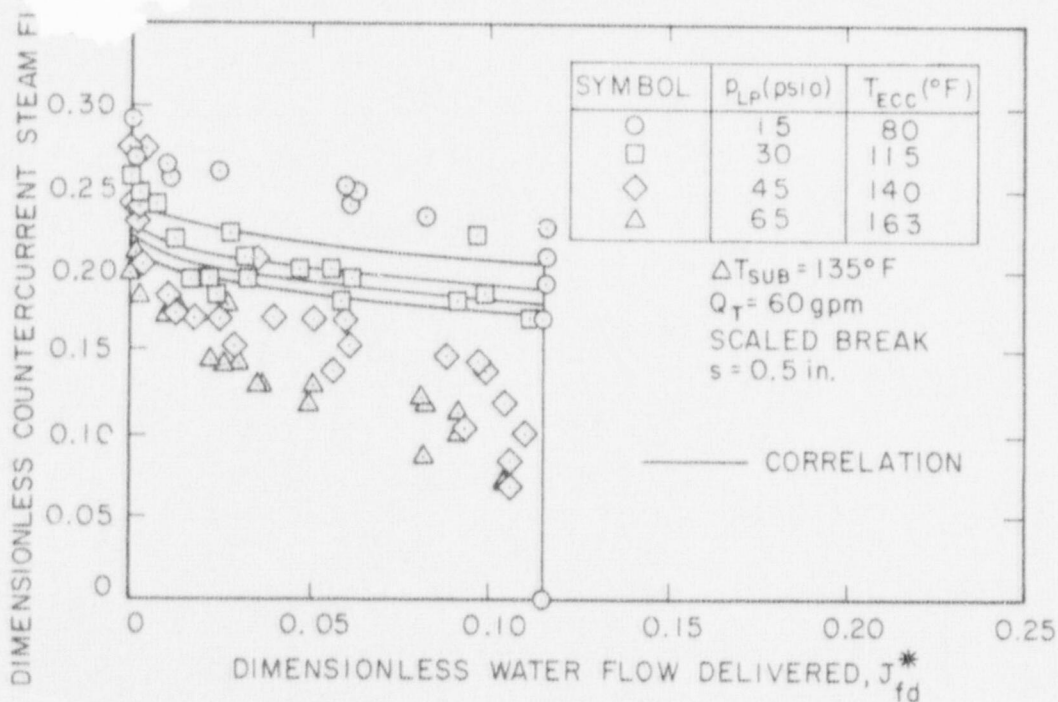


Figure 18. COMPARISON OF PREVIOUS CORRELATION [13] WITH CREARE 1/15-SCALE DATA FOR 135 $^{\circ}F$ ECC SUBCOOLING AT VARIOUS VESSEL PRESSURES

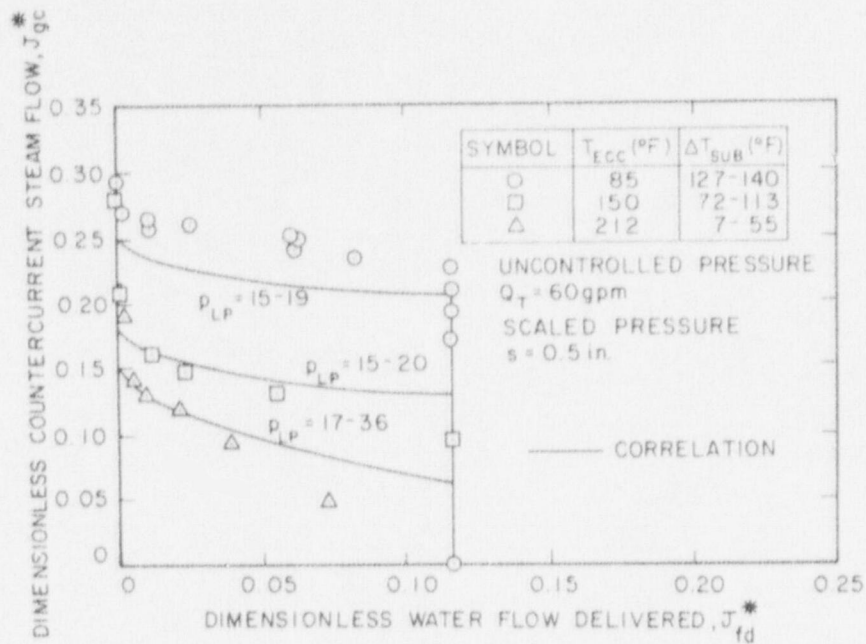


Figure 19. COMPARISON OF PREVIOUS CORRELATION [13] WITH CREARE 1/15-SCALE DATA FOR SUBCOOLED WATER AT VESSEL PRESSURES NEAR AMBIENT

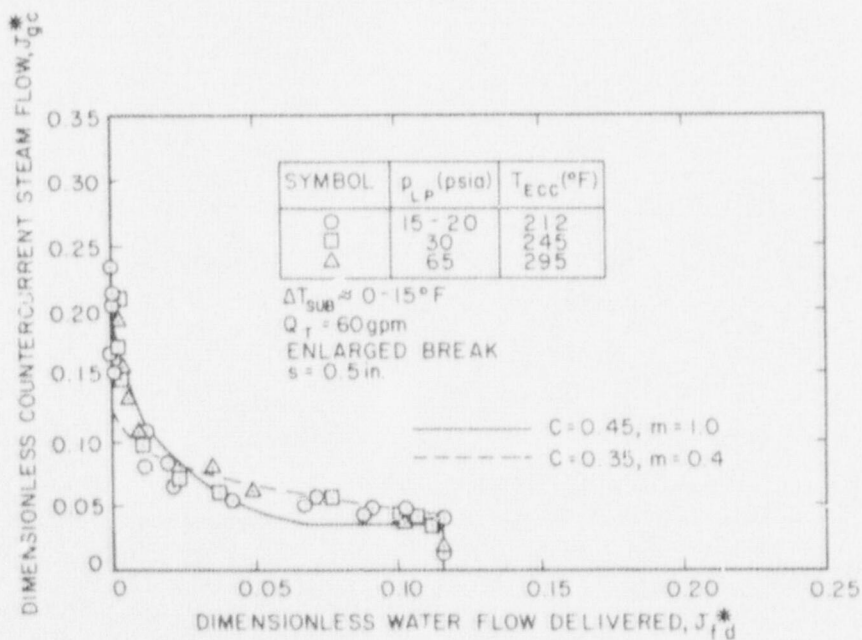


Figure 20. COMPARISON OF CORRELATIONS WITH CREARE 1/15-SCALE DATA SHOWING SENSITIVITY TO FACTORS C and m

The effect of condensation in the correlation through the condensation efficiency f is illustrated below. The recommended value of f is 0.16 for $J_{fin}^* = 0.116$. Figure 21 compares data near ambient pressure with the correlation for values of $f=0.1$ and 0.2 . Figures 22 and 23 are similar comparisons for data at a constant pressure of 65 psia (various subcoolings) and a constant subcooling of 125°F (various pressures) respectively. Most of the data are bounded by the correlation using these two values of the parameter f . The value of $f=0.16$ determined from statistical analysis of these data is therefore a good compromise over the range of these data. For certain values of the thermodynamic ratio ($R_{Td} \approx 1-1.5$) neither value of f appears quite adequate and some refinement of m (rather than f) might be desirable if greater accuracy were needed.

The various graphical comparisons in the preceding sections of this report supply considerable insight into the data trends. New correlation concepts have been proposed. These correlation concepts need to be extended to include the effects of ECC injection rate and the coefficients then need to be compared with the full data base and refined. Such comparisons should be both graphical and statistical.

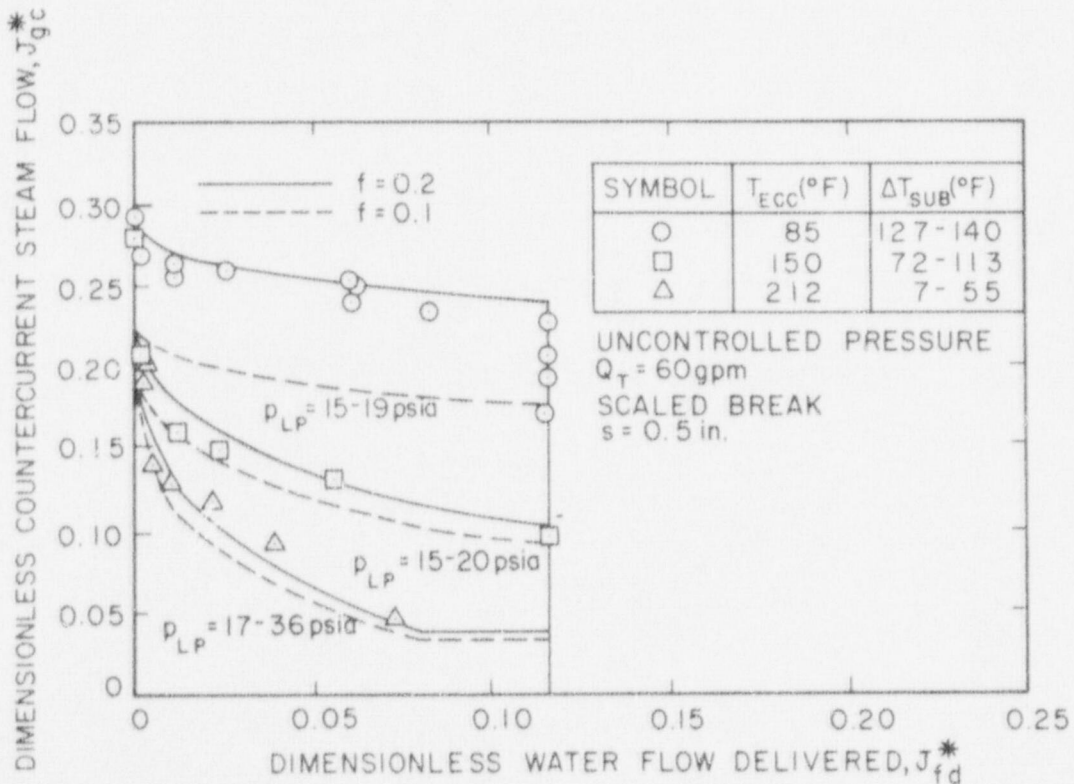


Figure 21. COMPARISON OF CORRELATIONS WITH CREARE 1/15-SCALE DATA SHOWING SENSITIVITY TO FACTOR f AT AMBIENT VESSEL PRESSURE

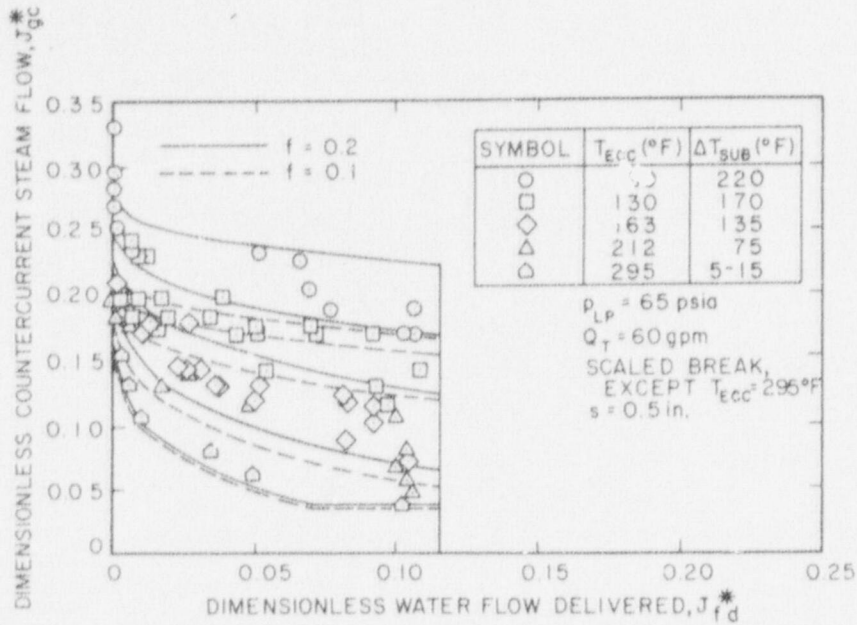


Figure 22. COMPARISON OF CORRELATIONS WITH CREARE 1/15-SCALE DATA SHOWING SENSITIVITY TO FACTOR f AT 65 PSIA VESSEL PRESSURE

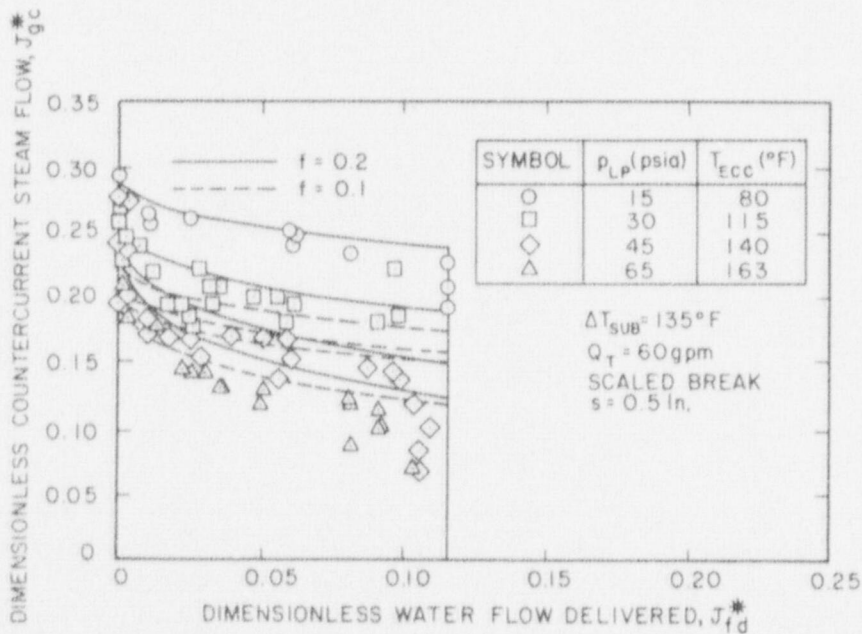


Figure 23. COMPARISON OF CORRELATIONS WITH CREARE 1/15-SCALE DATA SHOWING SENSITIVITY TO FACTOR f FOR 135 $^{\circ}F$ ECC SUBCOOLING

4 PROGRESS ON SCALING OF COUNTERCURRENT FLOW

In this section we address several interrelated scaling issues. Based on saturated-water data we assess appropriate dimensionless parameters for scaling flooding. Subcooled-water data are then used to tentatively assess the scaling of the effects of condensation on ECC bypass. The implications of our findings are discussed.

4.1 Scaling of Saturated-Water Behavior

Experiments have been conducted with vessels ranging from 1/30 to 2/15 of PWR diameter. Rothe et. al. [17] reported the status of scaling assessments based on tests with water near saturation temperature (or air-water tests). We simply update that detailed review here.

Figure 24 summarizes present knowledge of scaling of the complete bypass point for saturated water. Comparison with the earlier report (Figure 7 of Reference [17]) shows the loss of one data point and the addition of two others.

The point representing the Battelle 1/15-scale air-water data [3], which was inconsistent with all other data, has been discredited by test repetition at Battelle on three separate occasions. Unfortunately, data inconsistencies remain in the Battelle data sets and are still under study. Therefore, this point has been removed but cannot yet be replaced.

Collier [21] reports air-water and steam-water data at 2/15 scale. Figure 25 shows the steam-water data for nearly saturated water. (Numbers by the data points are the ECC subcooling.) Because this data set exhibits significant scatter and does not extend to complete bypass, additional saturated water data at this scale are desirable. Further tests are planned by Battelle. These data are reasonably represented by Equation (3) with $C=0.4\pm 0.06$ and $m=0.8\pm 0.2$. However, the uncertainty in the coefficient C is of the order of the difference between J^* and $K^*=3.2$ scaling. This uncertainty is a result of the large data scatter and the need to extrapolate to complete bypass. Figure 26 compares our correlation with these data and indicates that subcooling and injection rate are calculated to have little effect. Thus, the scatter reflects test repeatability.

Battelle is in the process of obtaining additional data to complete and confirm the set of initial 2/15-scale air-water data reported in Reference [21]. In discussions with Collier of Battelle we agreed that inclusion of the preliminary air-water data [21] on our scaling map would be premature.

Richter et. al. [22] report air-water data from a 1/10-scale annulus studied with top flood. Although ECC injection was not a feature of these experiments it is useful to compare them with other data (Figure 24). The data of Richter et. al. are shown in Figure 27 and are well fit by Equation (3) in the range near complete bypass. Values of $C=0.39\pm 0.01$ result. The data of Richter et. al. are also compared in Figure 28 with the Creare 1/15-scale saturated water data [17]. It may be seen that the two data sets are quite similar in appearance although the data of Richter are slightly lower. This small difference may be due to the slight subcooling in the steam-water experiments, a weak effect of asymmetrical injection or may very weakly suggest the beginning of a possible trend to K^* scaling.

An end-of-bypass transition of $J_{gC}^*=0.04$ is appropriate to all small-scale saturated water data obtained to date. However, it is uncertain how to extrapolate to PWR scale.

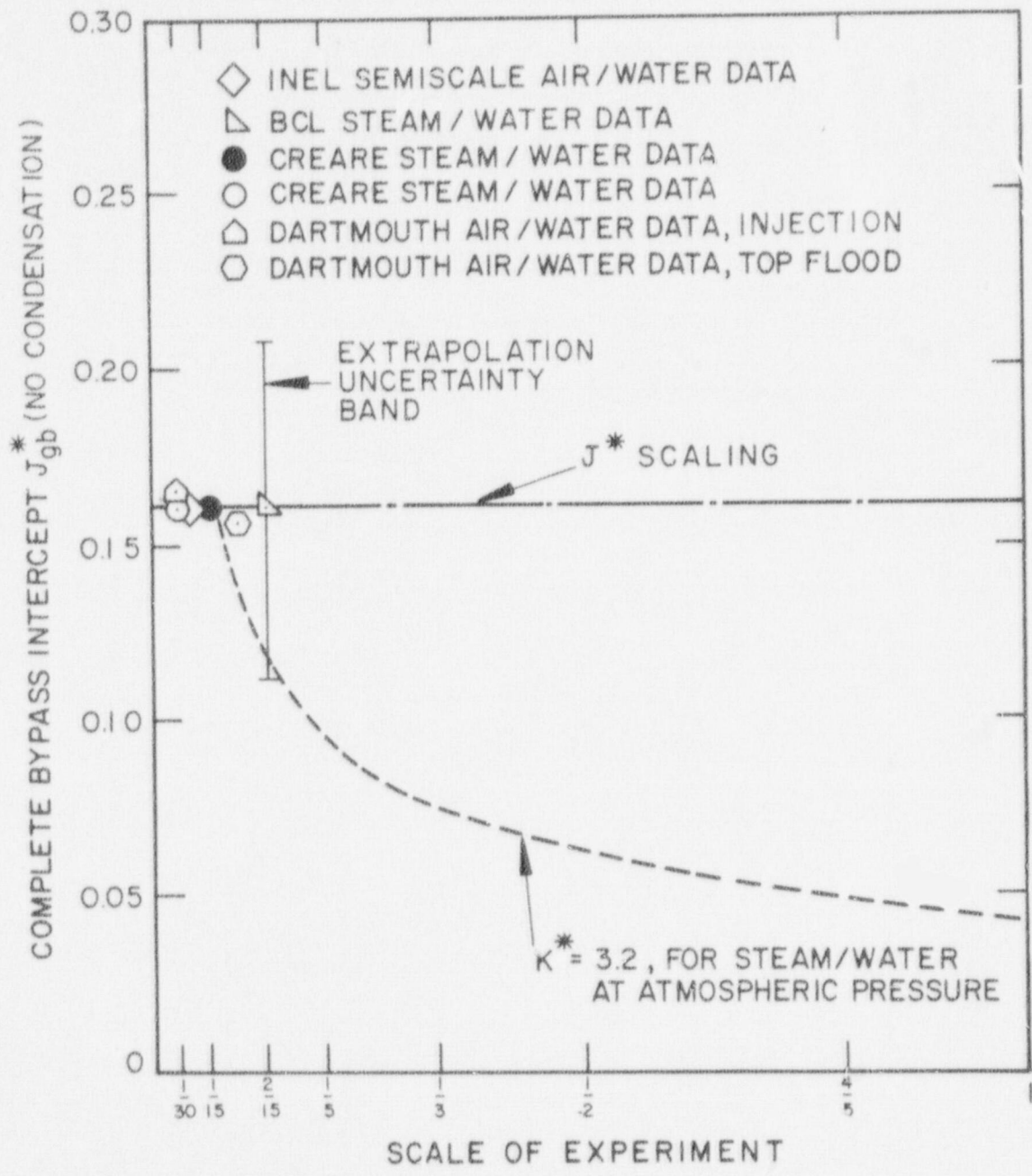


Figure 24. ECC BYPASS SCALING FOR SATURATED WATER

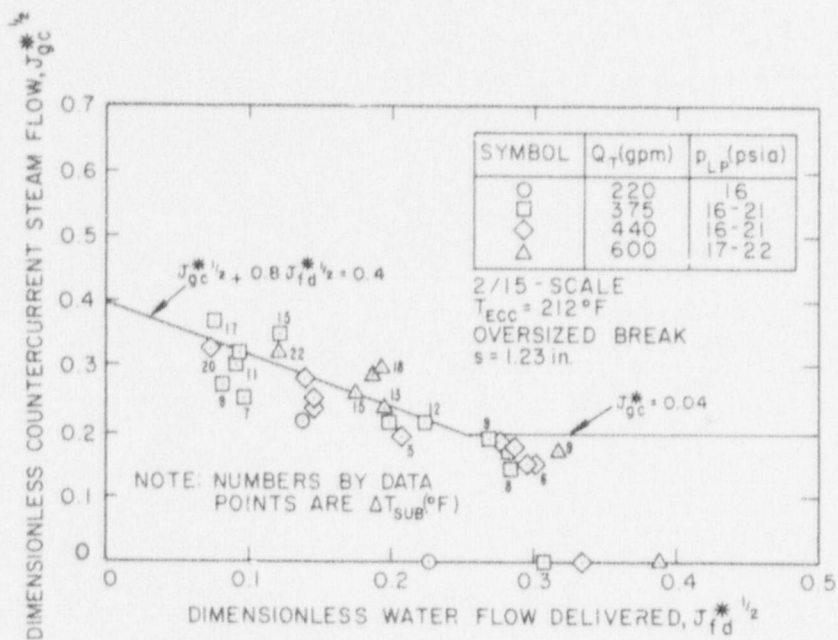


Figure 25. COMPARISON OF PRESENT SATURATED WATER CORRELATION WITH BATTELLE 2/15-SCALE DATA [21] SHOWING EXTRAPOLATION TO COMPLETE BYPASS

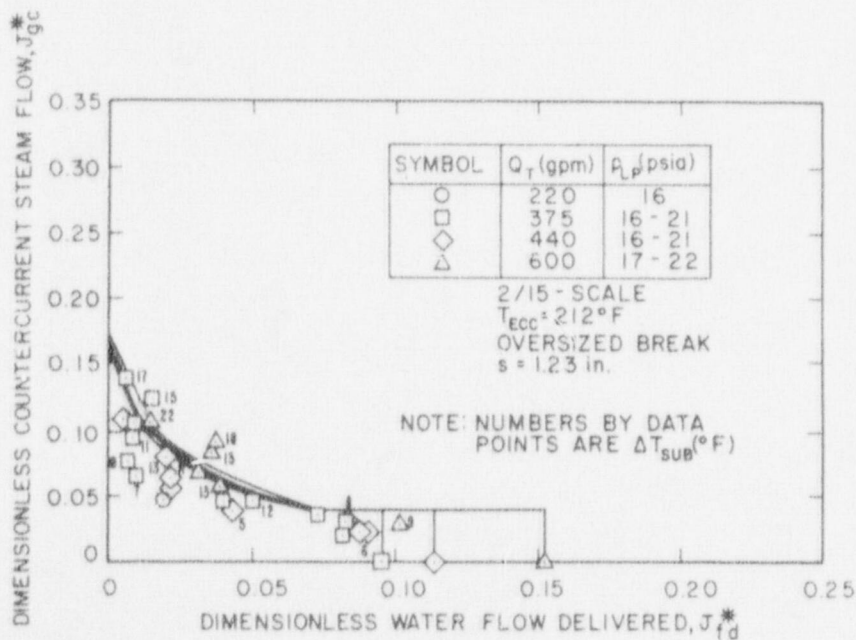


Figure 26. COMPARISON OF PRESENT CORRELATION WITH BATTELLE 2/15-SCALE DATA [21] FOR NEARLY SATURATED WATER SHOWING WEAK CALCULATED EFFECT OF SUB-COOLING AND INJECTION RATE RELATIVE TO DATA SCATTER

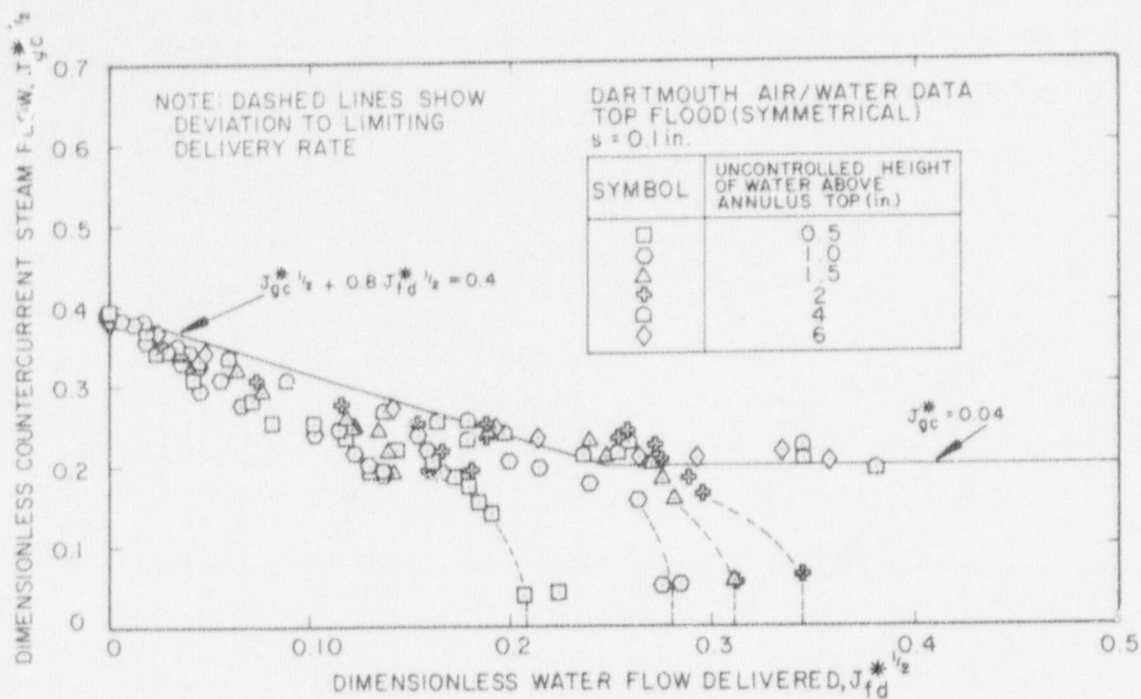


Figure 27. COMPARISON OF PRESENT CORRELATION WITH DARTMOUTH 1/10-SCALE AIR-WATER DATA [22]

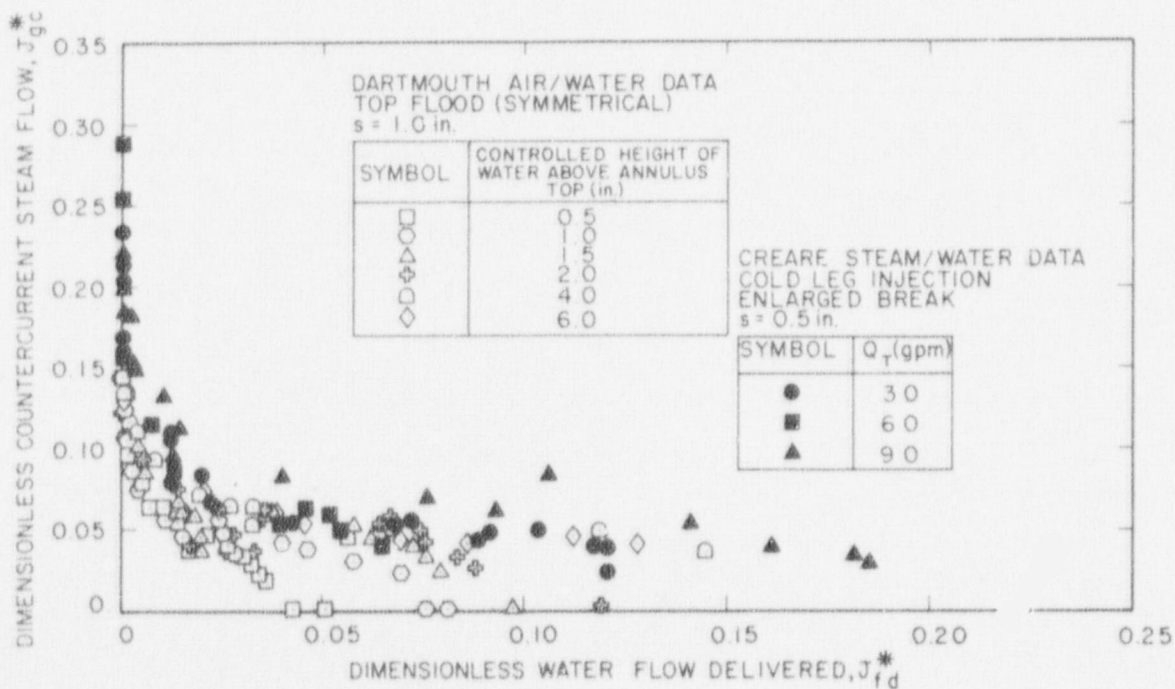


Figure 28. COMPARISON OF DARTMOUTH 1/10-SCALE AIR-WATER DATA [22] WITH CREARE 1/15-SCALE STEAM-WATER DATA FOR NEARLY SATURATED WATER [17]

Referring to Figure 24 we find that the conclusions of Reference [17] are unchanged by these additional data:

- 1) Flooding and countercurrent flow experiments are needed in facilities considerably larger than those in use today, which range from 1/30 to 2/15 of PWR scale, in order to answer scaling questions satisfactorily.
- 2) It is possible to unify existing saturated-water flooding data by the assertion that J^* scaling applies at small scales (where Kutateladze number is less than 3.2).
- 3) It is uncertain how flooding data should be extrapolated to scales larger than 1/15.

4.2 Preliminary Scaling Assessment of Subcooled Water Data

In this subsection we make a preliminary assessment of the data base available for scaling the effects of condensation. Figure 29 displays the factor "f" determined from subcooled water data at various scales.

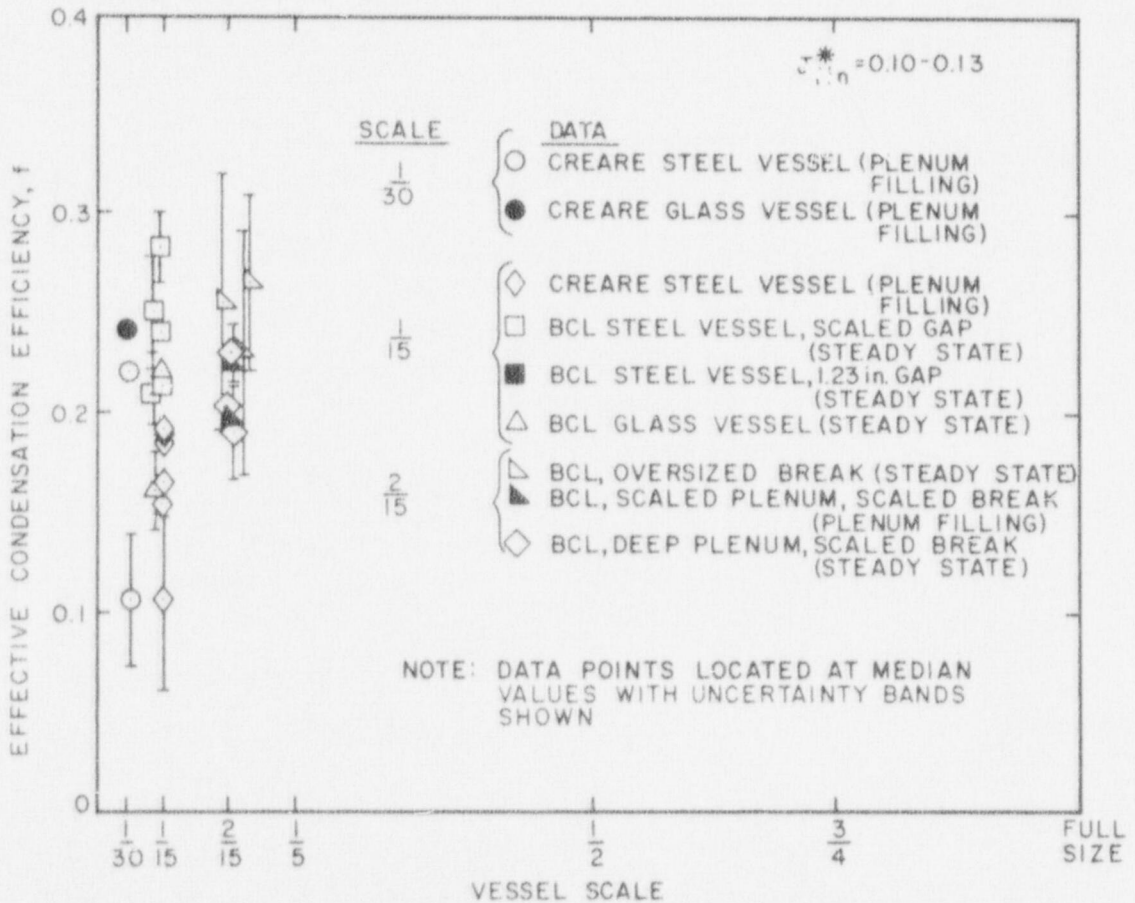


Figure 29. SCALING MAP FOR THE EFFECT OF CONDENSATION ON ECC BYPASS

Table 4 lists the available countercurrent flow data. However, certain facilities have not been represented on Figure 29 for various reasons. Dartmouth 1/30-scale data [25] do not extend to the desired range of injection rates. The Semiscale data [27] are difficult to compare with other data because the geometry is unusual, particularly there are two concentric gaps. CE 1/5-scale data have been excluded because sufficient data to determine f reliably are not available.

TABLE 4				
SUMMARY OF COUNTERCURRENT FLOW DATA				
Contractor	Scale	Gas	Subcooling	Reference
<u>Data on Saturated Water Behavior</u>				
Creare	1/30	Steam	$\approx 7^\circ\text{F}$	[15]
Creare	1/15	Steam	0-20 $^\circ\text{F}$	[17]
Dartmouth	1/30	Air	—	[23]
INEL	1/25	Air	—	[24]
Dartmouth	1/10	Steam	—	[22]
Battelle	1/15	Air	—	[3]
Battelle	2/15	Steam	$\leq 20^\circ\text{F}$	[21]
<u>Subcooled Countercurrent Flow Data</u>				
Dartmouth	1/30	Steam	15-170 $^\circ\text{F}$	[25]
Creare	1/30	Steam	7-150 $^\circ\text{F}$	[15]
Creare	1/30	Steam	0-135 $^\circ\text{F}$	[26]
INEL	1/25	Steam	20-90 $^\circ\text{F}$	[27]
Creare	1/15	Steam	10-135 $^\circ\text{F}$	[16]
Battelle	1/15	Steam	10-170 $^\circ\text{F}$	[6,8]
Battelle	2/15	Steam	110-235 $^\circ\text{F}$	[11,21]
CE	1/5	Steam	95-170 $^\circ\text{F}$	[28].
<u>Additional Saturated Water Data Expected</u>				
Battelle	1/15	Air	—	Unpublished
Battelle	2/15	Steam	$\leq 30^\circ\text{F}$	Planned
Battelle	2/15	Air	—	[21] (Under Study)

Each point in Figure 29 represents the complete bypass point for one delivery curve, i.e., for one facility, ECC subcooling, injection rate, and vessel pressure. The values of f have been calculated with the assumption that $C=0.40$ at all scales. All pressures and ECC subcoolings are represented in Figure 29 but we have restricted the injection rates to the range $0.10 < J_{in} < 0.13$. The interval shown for a few of the data points represents only the additional uncertainty introduced in determining the complete bypass point; the uncertainty of the delivery data themselves has not been included.

Figure 29 reveals that the factor f lies in the range $0.1 < f < 0.3$ in facilities from 1/30 to 2/15 of PWR scale. Within that range, the scatter in f obscures any likely dependence on scale. Based only on Figure 29, the factor f may be constant, a function of J_{fin}^* , or it may also depend on other dimensionless parameters or scale in some yet undetermined way.

Figure 29 is helpful because it summarizes a large body of data, but it is also misleading because it represents a number of geometries and test procedures. Some selected data comparisons follow.

Figure 30 compares Creare data at two scales for highly subcooled water. The difference between the two data sets is small. Data repetition might be desirable to confirm the accuracy of the 1/30-scale data which represent very early tests before definitive test procedures had been established.

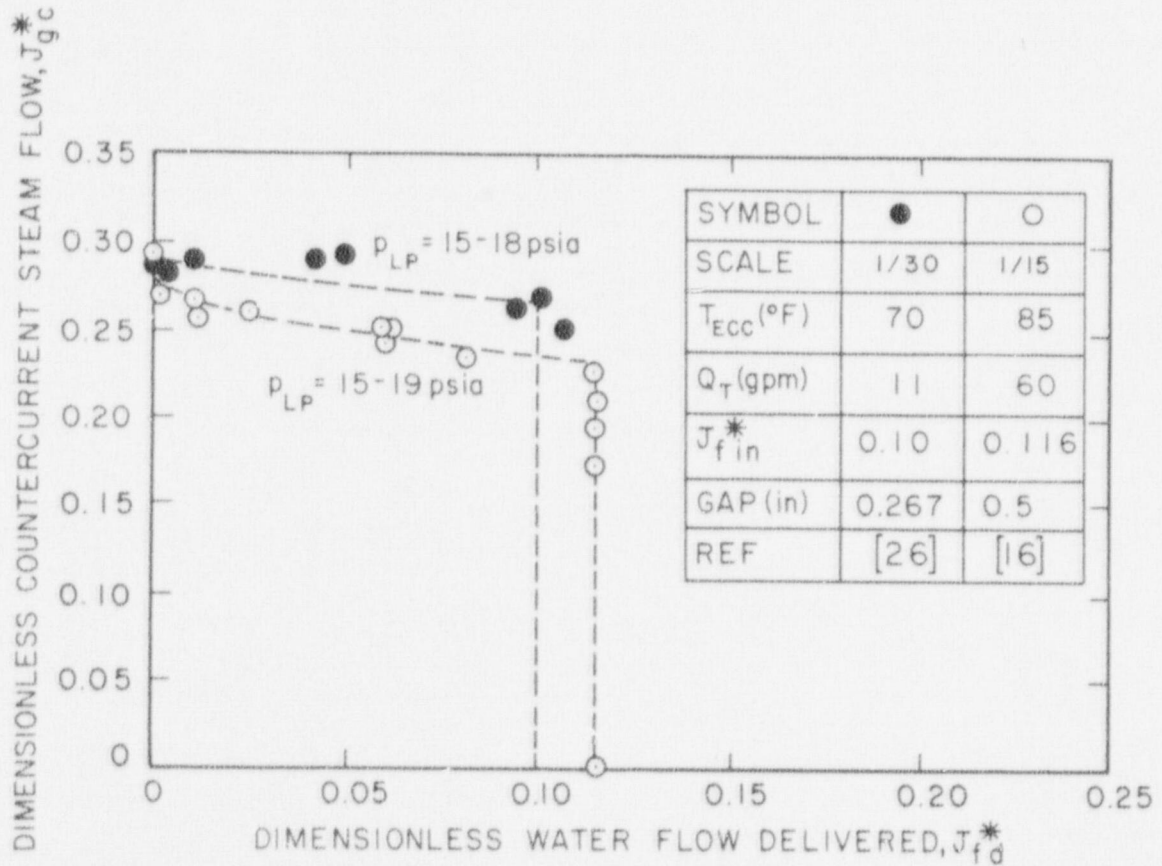


Figure 30. COMPARISON OF CREARE DATA AT 1/30 AND 1/15 SCALES FOR HIGHLY SUBCOOLED ECC

Figure 31 compares Battelle data at 1/15 and 2/15 scales. The solid symbols represent "steady-state" tests where the lower plenum liquid is pumped out and the operator attempts to manually hold the lower plenum liquid at a constant level by adjusting a valve. Since this procedure is known to introduce operator error and also alters the system dynamics [15], we have also compared these data with a set of Battelle "plenum filling" tests where the lower plenum drain is closed and the vessel simply fills up. Figure 31 shows that the data from the two scales overlay when the same (steady state) test procedure is followed. However, there is a marked difference between data obtained with the two test procedures. (There were no Battelle 1/15-scale data taken in the plenum filling mode under equivalent injection conditions.)

Figure 32 compares Creare 1/15-scale data with Battelle 2/15-scale data. Here again data at different scales overlay well as long as the tests were performed with the same test procedure. In this case only plenum filling data can be compared. (Believing that the steady-state mode is unreliable, Creare runs tests only in the plenum filling mode.) Figure 33 compares Battelle and Creare 1/15-scale data taken in the steady state and plenum filling modes respectively. As at 2/15 scale, the steady state data lie well above the plenum filling data. Battelle 1/15-scale plenum filling data at this injection rate are limited to a single point and have therefore not been included in this comparison. However, plenum filling data obtained by Battelle [33] at various injection rates are consistent with Creare plenum filling data, but are not compared directly here because corresponding data at the same injection rates are lacking.

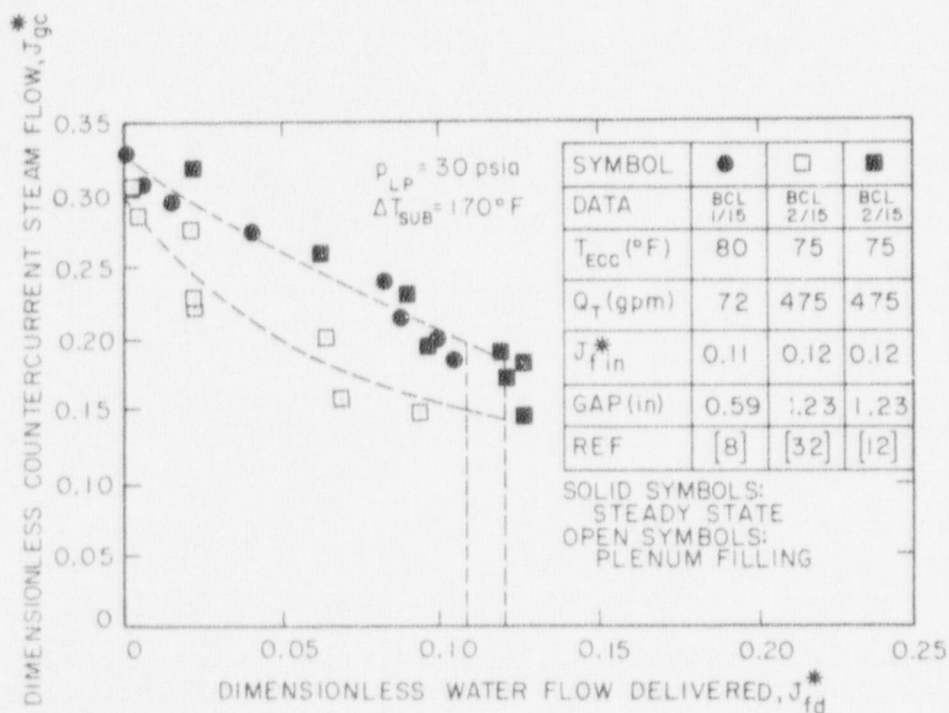


Figure 31. COMPARISON OF BATTELLE DATA FOR STEADY STATE AND PLENUM FILLING TEST MODES AT TWO SCALES

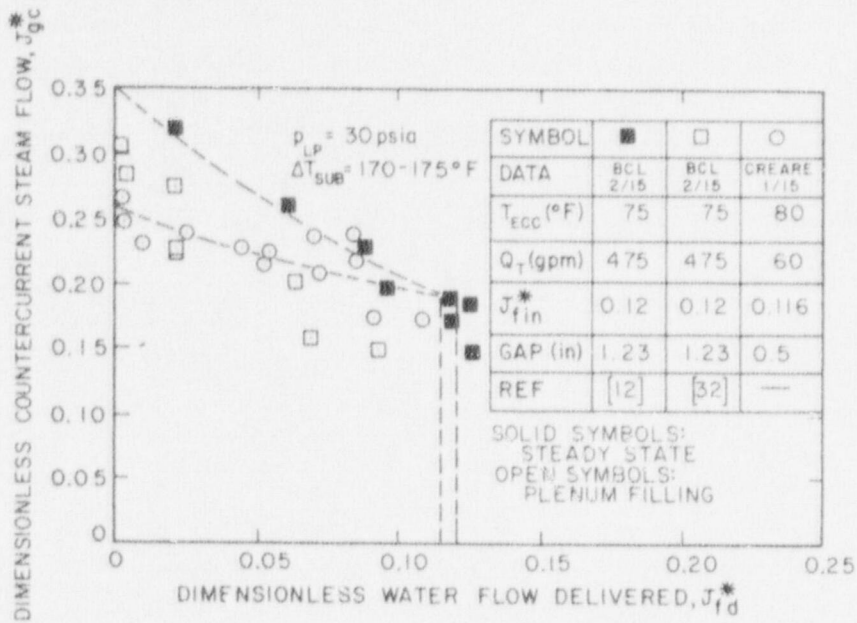


Figure 32. COMPARISON OF CREARE 1/15-SCALE AND BATTELLE 2/15-SCALE PLENUM FILLING DATA SHOWING DISAGREEMENT OF BOTH WITH BATTELLE STEADY-STATE DATA

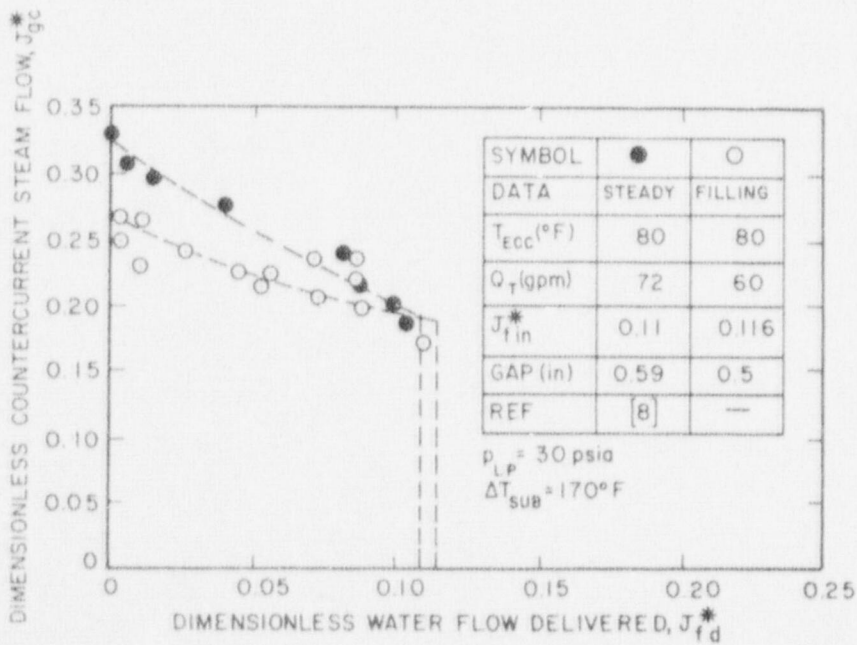


Figure 33. COMPARISON OF 1/15-SCALE DATA FOR PLENUM FILLING AND STEADY-STATE TEST MODES

In the interests of brevity we have included only the prime range of ECC injection rates in this assessment of data. The data at other injection rates are similar in content and trends.

The main purpose of this preliminary assessment of subcooled water has been to identify gaps in the data base for scaling the effects of condensation on counter-current flow. We conclude that:

- 1) the factor f is much smaller than the value unity given by simple "equilibrium" models; a value of 0.16 is appropriate for the data presented in this report,
- 2) the data base is large and displays considerable scatter in the factor f which obscures clear trends in f ,
- 3) for small 1/30 to 2/15-scale facilities, the correlation factor f may well be a constant, or at most a function of J_{tip}^* , but additional data will be needed to demonstrate this trend convincingly,
- 4) selected data comparisons suggest that the effects of condensation at different physical scales are indeed adequately accounted by representing the data on J^* coordinates, but here too additional data will be needed to make a convincing scaling demonstration,
- 5) data taken in the steady state mode differ significantly from plenum filling data, at all scales tested,
- 6) data obtained by different investigators using the same test model overlay well,
- 7) additional data at significantly larger scale are desirable.

5 SUMMARY OF SPECIFIC FINDINGS ON COUNTERCURRENT FLOW

Countercurrent flow data have been obtained and analyzed to study the separate processes of flooding (with saturated water) and condensation. A number of new data correlation concepts have been introduced in this report. These concepts have been shown to be useful by comparison with a selected body of data, taken over a very wide range of pressures and subcoolings, that we obtained specifically for this purpose. Further development and extension of these concepts and comparisons with all available data are needed.

Relative to flooding of saturated water we find that:

- 1) water delivery is insensitive to injection rate in the range $0.05 < J_{fin}^* < 0.20$,
- 2) water delivery is insensitive to vessel pressure in the range $15 < p_{LP} < 65$ psia,
- 3) an abrupt transition to full delivery at a steam or air flux of about $J_{gc}^* = 0.04$ has been observed in three independent facilities, at three different scales,
- 4) in the range from 1/30 to 1/15-scale, both the complete bypass points and the complete delivery limits are well represented by J^* scaling,
- 5) available 1/10-scale annulus data and 2/15-scale vessel data are consistent with J^* scaling, but the former data do not include ECC injection and the latter data are too limited and have excessive scatter to verify J^* scaling at 2/15 scale.

Relative to the additional effects of condensation on delivery, we find that:

- 6) a concept where the supplied steam flux J_{gc}^* is reduced due to condensation to an "effective" steam flux J_g^* continues to be an appropriate way to correlate data,
- 7) this steam flux "reduction", which has in the past been expressed as a function of thermodynamic ratio, pressure and injection rate, can be simplified to exclude pressure,
- 8) this concept has been demonstrated to the extent that data for various pressures and subcoolings can be represented by thermodynamic ratio rather than pressure or subcooling independently,
- 9) a particular correlation approach which involves sequential treatment of the complete bypass points and the partial delivery range has been useful in analyzing the data,
- 10) this approach leads to factors f representing the complete bypass points and m representing the slopes of the delivery curves which for a particular injection rate are respectively a constant and a function only of thermodynamic ratio.
- 11) however, available data for different water injection rates indicate possible additional effects of that parameter when there is condensation; these effects need to be incorporated in the correlation concepts as they have been in past correlations,
- 12) statistical studies by Battelle also suggest that the pressure could be excluded from the factor f ,

- 13) the Battelle correlation may be improved by refining m ,
- 14) if the data base is viewed in its entirety, there is far too much scatter to identify the proper scaling of the condensation factor f ,
- 15) however, selected comparisons of data obtained with similar test procedures suggest the possibility that f may depend only on J_{in}^* and thus may be otherwise independent of scale; additional data and data analysis are needed to verify this idea.

Relative to the availability of data necessary for analysis we find that:

- 16) extensive data are available at 1/30, 1/15 and 2/15 scales and that two investigators have independent sets of data at 1/15 scale,
- 17) there are important differences in testing modes which need to be considered in comparing data, particularly when assessing scaling,
- 18) additional data taken only in the plenum-filling mode are needed and should be compared independently from "steady-state" data,
- 19) independent comparisons of data taken only in the steady-state mode may also be useful if the data base is carefully restricted to recent tests where greater attention has been paid to level control,
- 20) some data have been obtained at vessel pressures near the boiler pressure where the steam supply is unchoked and hence unsteady; these data need to be isolated in data comparisons because it is not certain that they are equivalent to tests with steady steam flow,
- 21) the primary basis for data comparisons should be tests in the "controlled pressure" mode although tests with "uncontrolled pressure" are also important since they do not involve break variation or active pressure control and therefore help to validate the methods of controlling pressure,
- 22) very early data taken by all investigators (before proper test procedures were established) are suspect,
- 23) standard values of the main parameters have not been established, leading to slightly different conditions being tested at different scales,
- 24) recent data obtained by different investigators agreed closely as long as the tests were performed in the same mode and with the same values of the parameters,
- 25) additional 2/15-scale data for saturated water would be desirable,
- 26) recent 2/15-scale data with a scaled lower plenum are a good example of the ranges of subcoolings needed and available plenum filling data with a deep lower plenum should be extended to include this range,
- 27) extended ranges of injection rate at various pressures need to be tested at several facilities,
- 28) some additional data are needed at 2/15-scale to extend existing data sets to and beyond complete bypass,

Finally, we want to emphasize two key points. First, while an understanding of the physics may be generated more quickly and cheaply in small-scale facilities, there is a need for a few critical verification tests at significantly larger scale. Much of the value of the tests at small scale may be their contribution to the design of necessary larger facilities and test programs as well as the predictive tools they provide. Secondly, the data analysis in this report has revealed that subcooling may have much weaker effects on ECC bypass than suspected previously. The recommended value $f=0.16$ indicates a very weak effect of subcooling on complete bypass and the "slope factor" m representing the partial delivery range has been found to vary abruptly as a function of thermodynamic ratio. At reasonable values of pressure and subcooling, saturated-water data and subcooled water data are similar.

6 CONCLUDING REMARKS ON IMPLICATIONS OF FINDINGS

Preceding sections of this report have shown that the effects of ECC subcooling and vessel pressure need not be viewed independently, but can be treated more generally as effects of condensation. The degree of condensation and its effects on ECC bypass are well represented quantitatively by a correlating concept that relies on thermodynamic ratio.

At complete bypass the effect of condensation on ECC bypass is very weak. Data in this report indicate that suppression of ECC bypass by condensation may be represented by a value $f=0.16$ at 1/15 scale implying only 16% of the effect that would be calculated if thermodynamic equilibrium were achieved ideally. The ECC bypass data are also evidence of an abrupt transition in the countercurrent flow behavior near a thermodynamic ratio of 1 or 2. For thermodynamic ratios below the transitional value, the behavior is very near to that of saturated water. Insufficient data exist to confirm a definite value of the transitional thermodynamic ratio in available small scale experiments. Based on the limited available data, the transition appears to occur, for example, at an ECC subcooling of about 120°F for a vessel pressure of about 65 psia.

ECC supply temperatures in reactor accumulators are usually designed to be in the range 90 to 120°F. At even a moderate pressure of 65 psia this implies an ECC subcooling entering the cold leg of about 200°F. However, the ECC is calculated to be heated significantly when it enters the cold legs due mainly to condensation of the steam flowing through the cold legs but also due to heat transfer from piping. ECC temperatures entering the annulus may even approach saturation temperatures, as has been observed repeatedly in the Semiscale facility (tests S-06-J to S-06-6 for example). Even if the ECC temperature is somewhat subcooled, we now know that it must be significantly subcooled, in excess of the transitional thermodynamic ratio, for there to be significant suppression of ECC bypass by the condensation.

Methods to confidently scale condensation rates or their effects have not yet been developed [19,29]. Moreover, Section 4.2 shows that the proper scaling of condensation effects on ECC bypass has not yet been established even for the 1/30 to 2/15-scale range where small scale data exist. Plainly this latter situation needs to be improved, but the more fundamental issue of extrapolating to larger scale from the small scale tests will not be satisfactorily addressed until at least a few critical verification data have been obtained at larger scale.

Taken together, the above factors lead us to suggest that in bounding calculations of refill following a postulated LOCA, it would be prudent to take no credit for the possible benefits of ECC subcooling with respect to ECC bypass. However, the effects of ECC subcooling should be included in the calculation of annulus steam flow with appropriate allowances to account for uncertainties in modeling condensation. In the development of best-estimate LOCA analyses, attention should be given to incorporating the small-scale behavior described here.

REFERENCES

- 1) Block, J. A. and Schrock, V. E.; EMERGENCY COOLING WATER DELIVERY TO THE CORE INLET OF PWR's DURING LOCA; Paper published in Thermal and Hydraulic Aspects of Nuclear Safety, Light Water Reactors, Vol. 1, p. 109, November 1977.
- 2) Crowley, C. J. et. al.; STEAM/WATER INTERACTION IN A SCALE PRESSURIZED WATER REACTOR DOWNCOMER ANNULUS; Thayer School of Engineering, Rep. No. COO-2294-4, September 1974.
- 3) Cudnik, R. A. and Wooton, R. O.; PENETRATION OF INJECTED ECC WATER THROUGH THE DOWNCOMER ANNULUS IN THE PRESENCE OF REVERSE CORE STEAM FLOW; Status Report, Battelle Columbus Laboratories, November 1, 1974.
- 4) Wallis, G. B. and Crowley, C. J.; COMPARISON OF BATTELLE GLASS VESSEL PRELIMINARY DATA WITH 1/30 SCALE STEAM/WATER INTERACTION RESULTS OBTAINED AT DARTMOUTH; AEC, Creare Technical Memorandum TM-353, October 1974.
- 5) Block, J. A. and Crowley, C. J.; EFFECTS OF STEAM UPFLOW AND SUPERHEATED WALLS ON ECC DELIVERY IN A SIMULATED MULTILoop PWR GEOMETRY; NRC Quarterly Progress Report, Creare Technical Note TN-210, May 1975.
- 6) Flanigan, L. J., et. al.; EXPERIMENTAL STUDIES OF ECC DELIVERY IN A 1/15-SCALE TRANSPARENT VESSEL MODEL; Topical Report, Battelle Columbus Laboratories, BMI-1941, November 1975.
- 7) Cudnik, R. A., et. al.; STEAM-WATER MIXING AND SYSTEM HYDRODYNAMICS PROGRAM; Quarterly Progress Report, Battelle Columbus Laboratories, BMI-NUREG-1964, December 1976.
- 8) Cudnik, R. A., et. al.; PENETRATION BEHAVIOR IN A 1/15-SCALE MODEL OF A FOUR-LOOP PRESSURIZED WATER REACTOR; Topical Report, Battelle Columbus Laboratories, BMI-NUREG-1973, June 1977.
- 9) Carbiener, W. A., et. al.; STEAM-WATER MIXING AND SYSTEM HYDRODYNAMICS PROGRAM; Quarterly Progress Report, Battelle Columbus Laboratories, BMI-NUREG-1979, September 1977.
- 10) Carbiener, W. A., et. al.; STEAM-WATER MIXING AND SYSTEM HYDRODYNAMICS PROGRAM; Quarterly Progress Report, Battelle Columbus Laboratories, BMI-NUREG-1987, December 1977.
- 11) Carbiener, W. A., et. al.; STEAM-WATER MIXING AND SYSTEM HYDRODYNAMICS PROGRAM; Quarterly Progress Report, Battelle Columbus Laboratories, BMI-1993, NUREG/CR-0034, March 1978.
- 12) Cudnik, R. A., et. al.; BASELINE PLENUM FILLING BEHAVIOR IN A 2/15-SCALE MODEL OF A FOUR LOOP PRESSURIZED WATER REACTOR; Topical Report, Battelle Columbus Laboratories, BMI-1997, NUREG/CR-0069, April 1978.
- 13) Block, J. A., Rothe, P. H., Fanning, M. W., Crowley, C. J. and Wallis, G. B.; ANALYSIS OF ECC DELIVERY; Creare Technical Note TN-231, April 1976.
- 14) Block, J. A. and Crowley, C. J.; HOT WALL EXPERIMENTS IN A SIMULATED MULTILoop PWR GEOMETRY; Creare Technical Note TN-202, February 1975.

- 15) Rothe, P. H., Wallis, G. B. and Block, J. A.; A PRELIMINARY STUDY OF ANNULUS ECC FLOW OSCILLATIONS; Creare Technical Memorandum TM-517, November 1976, (also EPRI NP-839).
- 16) Crowley, C. J., Block, J. A. and Cary, C. N.; DOWNCOMER EFFECTS IN A 1/15-SCALE PWR GEOMETRY--EXPERIMENTAL DATA REPORT; Creare Technical Note TN-252, (NUREG-0281), February 1977.
- 17) Rothe, P. H., Crowley, C. J. and Block, J. A.; PROGRESS ON ECC BYPASS SCALING; Quarterly Progress Report, October 1, 1977 - December 31, 1977, Creare Technical Note TN-272, (NUREG/CR-0048), March 1978.
- 18) Block, J. A. and Crowley, C. J.; EFFECT OF ELEVATED PRESSURE ON ECC DELIVERY IN A SIMULATED PWR GEOMETRY; Quarterly Progress Report, July 1 - September 31, 1975, Creare Technical Note TN-224, October 1975.
- 19) Jones, W. C., Jr. and Saha, P.; NON-EQUILIBRIUM ASPECTS OF WATER REACTOR SAFETY; Paper published in Thermal Aspects of Nuclear Reactor Safety, Light Water Reactors, Vol. 1, p. 249, November 1977.
- 20) Rothe, P. H., Wallis, G. B. and Block, J. A.; COLD LEG ECC FLOW OSCILLATIONS; Paper published in Thermal and Hydraulic Aspects of Nuclear Reactor Safety, Light Water Reactors, Vol. 1, p. 133, November 1977.
- 21) Collier, R. P.; PRELIMINARY DATA REPORT FOR 2/15-SCALE MODEL DEVELOPMENT TESTS; Battelle Columbus Laboratories, June 5, 1978.
- 22) Richter, H. J., Wallis, G. B. and Speers, M. S.; EFFECT OF SCALE ON TWO-PHASE COUNTERCURRENT FLOW FLOODING; Thayer School of Engineering, Dartmouth College, NUREG/CR-0312, June 1978.
- 23) Graham, G.; SUMMARY OF RECENT THAYER SCHOOL ANNULUS PENETRATION RESULTS; Memorandum, Thayer School of Engineering, Dartmouth College, May 20, 1975.
- 24) Hanson, D. J.; EXPERIMENTAL DATA REPORT FOR SEMISCALE TRANSPARENT VESSEL COUNTERCURRENT FLOW TESTS; Aerojet Nuclear Company Report ANCR-1163, October 1975.
- 25) Graham, G. J.; TWO-PHASE FLOW IN A MODEL PRESSURIZED WATER REACTOR EQUIPPED WITH VENT VALVES; Thesis for Master of Engineering, Dartmouth College, Thayer School of Engineering, August 1976.
- 26) Crowley, C. J., Block, J. A. and Rothe, P. H.; AN EVALUATION OF ECC PENETRATION DATA USING TWO SCALING PARAMETERS; Creare Technical Note TN-233, September 1976.
- 27) Hanson, D. J., et. al.; ECC PERFORMANCE IN THE SEMISCALE GEOMETRY; Aerojet Nuclear Company, ANCR-1161, June 1974.
- 28) Brodrick, J. R., Loiselle, V.; ANNULUS PENETRATION TESTS; Nuclear Power Systems, Combustion Engineering, Windsor, Connecticut, AEC-CCO-2244-1, CENPD-130, March 1974.
- 29) Wallis, G. B., et. al.; AN EVALUATION OF PWR STEAM GENERATOR WATERHAMMER; Creare Technical Note TN-251, NUREG-0291, June 1977.
- 30) Block, J. A., Crowley, C. J. and Stacy, W. D.; CREARE 1/15-SCALE CYLINDRICAL ELEVATED PRESSURE FACILITY DESCRIPTION; Quarterly Progress Report, October 1 - December 31, 1975, Creare Technical Note TN-229, February 1976.

- 31) Collier, R. P.: PRELIMINARY DATA REPORT FOR 2/15-SCALED LOWER PLENUM DETAILED TRANSIENT TESTS; Battelle Columbus Laboratories, August 30, 1978.
- 32) Cudnik, R. A., et. al.; STEAM-WATER MIXING AND SYSTEM HYDRODYNAMICS PROGRAM, TASK FOUR; Battelle Columbus Laboratories Report BMI-2003, NUREG/CR-0147, June 1978.

APPENDIX A

DETAILED LITERATURE REVIEW

Rothe et. al. [17] reviewed the principal countercurrent flow data available up to March 1978. Therefore, this review focuses on efforts to correlate the data and updates the earlier review.

A.1 Correlations for Air/Water in Tubes

Wallis [A-1] first correlated countercurrent flow data in 1961. He studied flooding in vertical tubes for a limited range of diameters D (1/2 inch to 2 inches) using air and water at atmospheric pressure. He correlated his results with the equation

$$j_g^* + m j_f^* = C \quad (A1)$$

in which

$$j_g^* = j_g \rho_g^{1/2} [gD(\rho_f - \rho_g)]^{-1/2} \quad (A2)$$

$$j_f^* = j_f \rho_f^{1/2} [gD(\rho_f - \rho_g)]^{-1/2} \quad (A3)$$

The coefficient m was unity and the coefficient C varied depending on the end conditions, being 0.725 for sharp-edged flanges and 0.875 for smooth flanges, with some scatter in between. In this formulation j_g and j_f are the superficial velocities of the gas and liquid respectively. Present correlations have maintained this general form.

Over the years there have been efforts to justify Equation (A1) or the use of j^* parameters in similar formulations [A-2]. However, the main justification has been that it works; it fits data well.

Later studies by Pushkina and Sorokin [A-3], Wallis and Makkenchery [A-4], and Richter and Lovell [A-5] showed that Equation (A1) does not always work, particularly to correlate several sets of data from tubes with diameters in the range 2 to 1 1/2 inches. (The j^* parameters work well for tube diameters less than 2 inches.) Pushkina and Sorokin [A-3] proposed the correlation $K^* = 3.2$ where K^* is the Kutateladze number given by:

$$K^* = j_g \rho_g^{1/2} [g\sigma(\rho_f - \rho_g)]^{-1/2} \quad (A4)$$

Wallis and Kuo [A-6] give some additional theoretical justification for the use of K^* as a scaling parameter. Figure A1 shows the data comparison presented by Wallis and Makkenchery where $D^* = D[g(\rho_f - \rho_g)/\sigma]^{1/2}$ is a dimensionless diameter, the square root of the Bond number.

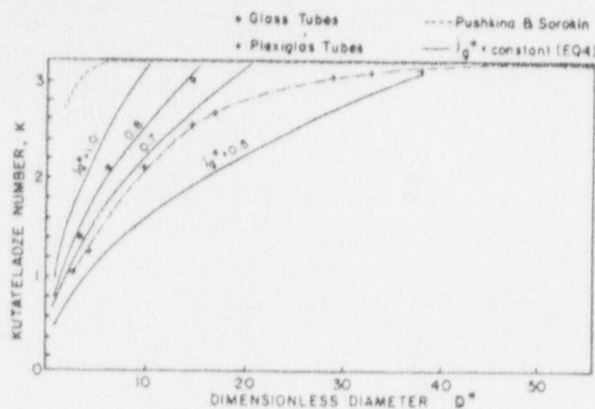


Figure A1. CRITICAL KUTATELADZE NUMBER (DIMENSIONLESS GAS FLUX) BELOW WHICH THE LIQUID FILM WILL FLOW DOWNWARDS

Recently Dukler [A-7] and Richter et. al. [22,A-5] have developed analyses of the countercurrent flow situation for air and water. These analyses support the use of K^* parameters to scale complete bypass. (Reference [A-5] also provides a method for predicting the penetration curves.) However, these analyses are dependent on assumptions of flow regime. Specifically, droplet and film flow regimes have been used based on observations in tubes with very low water flow rates [A-5,A-7]. However, these flow regimes have not generally been observed in tests in reactor vessel models with annular geometries, ECC injection and intense condensation [6,15,A-8]. Therefore, some additional analysis is needed to predict the flow regimes under various conditions and to predict countercurrent flow behavior for all relevant flow regimes.

This brief history serves to point out the difficulty in deriving reliable correlations. Almost two decades have been spent studying the "simple" situation of countercurrent flow in a vertical tube. The basic dimensionless parameters and methods of analysis are emerging very slowly due to the multiplicity of possible flow regimes as scale is varied. Real advances have been driven mainly by the acquisition of new data taken over a broader range of geometries. We should expect a similar situation in our efforts to correlate data from model reactor vessel geometries at elevated pressure and with injection of subcooled ECC (key factors underlined).

A.2 Correlation of Model Reactor Vessel Geometries

Distortion of the physics is inherent in most subscale model testing. In an effort to compensate for this and to build understanding of the physics, tests have been conducted in various distorted geometries. The reference geometry is linearly scaled--all dimensions are reduced by a common factor. Apart from vessel scale, geometric parameters have included:

- 1) annulus gap size,
- 2) annular or unwrapped (planar) downcomer,
- 3) broken leg diameter,
- 4) lower plenum depth (or volume),
- 5) intact cold leg diameter,
- 6) lower annulus depth,
- 7) upper annulus height,

- 8) cold leg arrangement, and
- 9) annulus obstructions.

Correlation of geometry has centered on the proper choice of dimensionless parameter rather than development of equations to account for each parameter. Knowledge of the effect of each parameter is reviewed briefly below.

Effect of Annulus Gap

Early work at Dartmouth College [2], Battelle [3] and Creare [4] reported data in terms of a parameter similar to that used for tubes:

$$j_x^* = \frac{\rho_x^{1/2} j_x}{[g D_h (\rho_f - \rho_g)]^{1/2}} \quad (A5)$$

where the subscript x can designate either the gas phase g or the liquid phase f. D_h is the hydraulic diameter of the annulus, $D_h = 2s$.

However, experiments by Block and Crowley [5] in early 1975 demonstrated conclusively that j_x^* parameters were not the appropriate dimensionless parameters to use to correlate countercurrent flow data. They chose instead to use the vessel circumference w as the characteristic dimension and they proposed the parameter:

$$J_x^* = \frac{\rho_x^{1/2} j_x}{[gw(\rho_f - \rho_g)]^{1/2}} \quad (A6)$$

Figures 6 and 11 of Reference [A-9] illustrate the data in j_x^* and J_x^* coordinate and demonstrate the superiority of the J_x^* coordinates.

These experiments were performed in a planar unwrapped annulus (parallel flat plates) at atmospheric pressure. The gap was varied from 0.25 to 2.0 inches. It should be noted that the gap plays a role in both the j_x^* and J_x^* parameters since it is used to calculate the superficial gas velocity j_g from the measured gas mass flow W_g according to:

$$j_g = W_g / \rho_g s w \quad (A7)$$

It should also be pointed out that the choice of w in J_x^* was arbitrary; other dimensions such as vessel diameter D_v or even annulus length L could have been chosen with equal validity.

Hanson [27] also found that the j_x^* parameters did not correlate data in the Semi-scale facility. He chose to simply remove the gap from the j_x^* parameters by reporting data in terms of the product $j_x^* D^{*1/2}$.

In 1976 Block and Crowley [A-9] and Block et. al. [13] showed the J_x^* parameters also successfully correlated data from a 1/15-scale cylindrical vessel (at elevated pressures) with gaps of 0.5 and 1.0 inch.

Cudnik et. al. [A-10] later supported this conclusion by similar tests in a 1/15-scale cylindrical vessel with gaps of 0.59 and 1.0 inch. Their correlation of these data [7] also artificially removed dependence on the gap, but was cast in terms of j_x^* parameters.*

Richter et. al. [22] recently reported air-water tests in a transparent annulus fed water from a pool at its top. The annulus was about 1/10 of PWR diameter and gaps of 1.0 inch and 2.0 inch were tested. With respect to the effect of the gap, these data are unacceptably correlated by the j_x^* parameters. The two sets of data at different gaps overlay well on J_x^* coordinates.

All available data refute the use of j_x^* parameters as coordinates to collapse data from otherwise identical vessels differing only in annulus gap. The available data support the use of various parameters or correlations which remove the effect of gap in a manner equivalent to the J_x^* parameters.

Downcomer Configuration

Extensive tests have been performed in both annular and planar (unwrapped annulus) geometries at 1/30 and 1/15 scale. The planar vessel data [2,33] display the same qualitative trends with all parameters as those exhibited by the annular vessel data [9,12,16]. However, the planar geometry tends to enhance delivery relative to comparable tests with an annular geometry and all other parameters the same [A-12].

Because the body of annular vessel data now exceeds that of the planar tests and the annular configuration more closely approximates reactor geometries, we are using the annular-vessel data as the primary data set for development of correlations. In particular, the annular vessel data include larger ranges of vessel scale, pressure, and subcooling than do the planar vessel data. The planar vessel data are useful as a check on parameter trends and also include certain key data such as those showing the effect of gap. The planar geometry is also simpler in some respects and therefore has advantages for comparison with analyses and numerical models such as K-TIF.

Effect of Broken Leg Diameter

Broken leg geometry has been varied at several facilities [12,16,17,21] using various methods to both increase and decrease break size. As expected, reduced break size increases the time-average pressure difference between the vessel and containment. Believing that it is the vessel pressure that governs processes in the vessel, parallel tests performed with different breaks have been controlled to the same vessel pressure. (The containment pressure has been adjusted as required.) Under those conditions, break size has had little or no effect on countercurrent flow penetration curves as seen for example in Figures 22-24 of Reference 16 and Figure A2.

Battelle data and correlations were presented in j_x^ coordinates until 1978 [8] when they switched to J_x^* coordinates. Their early conclusions supporting the use of j_x^* parameters, e.g., Reference [A-11], should be interpreted in the context of the correlation in use at that time. Specifically, the dependence on gap was removed so that it was functionally equivalent to the use of J_x^* parameters with respect to dependence on gap.

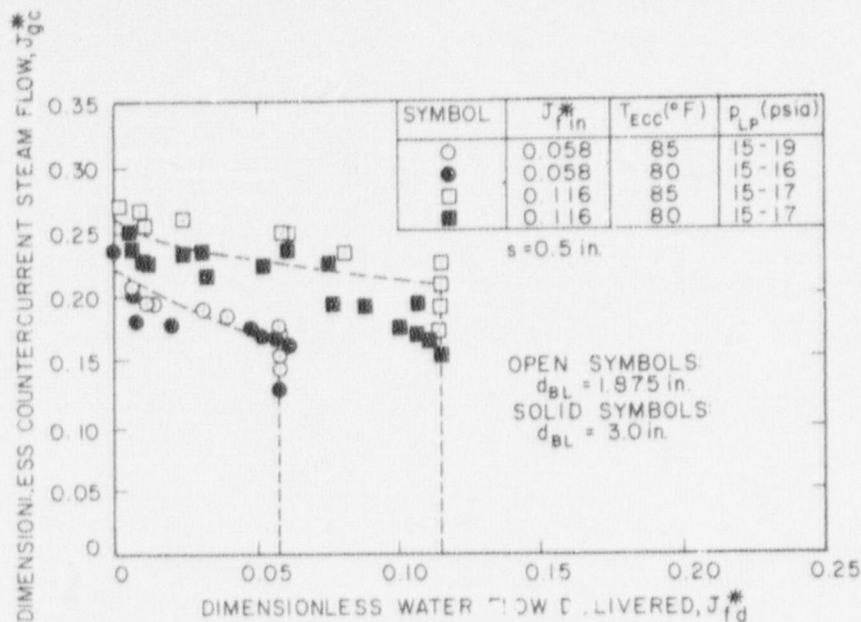


Figure A2. COMPARISON OF CCF DATA FOR TWO BREAK SIZES AT 1/15-SCALE

Effect of Lower Plenum Depth

Reference [16] compares tests with scaled (2 gal.) and deep (15 gal.) lower plenums. There is little or no effect of the lower plenum depth in those tests where delivery is steady. (Specifically, steady delivery occurs in tests with 212°F ECC or regardless of ECC temperature in tests with either complete bypass or nearly complete penetration.) However, larger plenum size enhances delivery slightly when slug delivery occurs--i.e., in tests in the partial penetration range with highly subcooled ECC.

Despite this slight difference, the lower plenums are interchangeable to first order. The deep lower plenum offers the important advantage of a longer test duration which leads to more reliable tests and reduces data uncertainty. Thus, we tend to favor these data in deriving correlations to assess the effects of other parameters.

Additional Geometric Parameters

Reference [16] reports tests over a factor of 4 range of cold leg diameter (a factor of 250 range of injected momentum). Figures 25 and 26 of Reference [16] show typical data which have little or no effect of cold leg diameter.

Annular length was varied by Crowley [2] in a 1/30-scale planar facility. He found little or no effect on ECC delivery. Annulus length was also a parameter in early tests with superheated walls in the Creare planar facility [A-13]. Additional tests of annulus length effects are underway in the 2/15-scale facility at Battelle. Hanson [27] also found that upper annulus length had no effect on delivery in the Semiscale geometry.

Alternate cold leg arrangements have been studied by Crowley [2], Cudnik et. al., [8] and Cudnik and Wooton [3] with mixed results. In some tests [2,3] a weak effect has been indicated, but more recent data (Figure 13 from Reference [8] for example) show no effect; if there is an effect, it lies well within data scatter (Figure 14. from Reference [8]).

Annulus obstructions have included hot leg plugs [8], a matrix of pins [8], baffles of various geometry [16,33] and lower plenum hardware [8,A-14]. The pins enhance bypass by reducing the downcomer cross-section and the baffles tend to suppress bypass by directing the liquid downward. The hot leg plugs and lower plenum hardware have little or no effect.

The above "additional" geometric parameters have in common their dependence on liquid momentum. Since cold leg diameter (which strongly and directly affects ECC injection momentum) has little effect, it is not surprising that parameters such as annulus length, hot leg plugs, or cold leg arrangement also have weak or no effects. Those parameters such as pins and baffles which have significant effects do so by altering the gas flow.

Summary of Geometric Effects

Although a large number of geometric parameters have been studied extensively, most have had little impact on efforts to correlate the data. We have learned that a deep lower plenum is helpful to get reliable data and that a large break is useful to help control vessel pressure. We have found that the annulus gap is not an appropriate dimension to use as a length scale to characterize ECC bypass. Finally, we have found that we lack a reliable method to extrapolate to PWR scale using present data from vessels in the range 1/30 to 2/15 of PWR scale.

A.3 Effects of Thermal and Hydraulic Parameters

Since the countercurrent flow data are reviewed in the body of the report, this section of the Appendix concentrates on the history of correlation development. By identifying correlation difficulties faced in early work we hope to place present modeling approaches in a broader perspective.

In the earliest work [2,3,4], there were few data and the main effort was to explain the basic behavior. A 1974 Battelle report [3] suggested direct use of the Wallis correlation:

$$j_g^{*2} + m j_L^{*2} = C \quad (A8)$$

with $C=0.8$ to 1.0 and $m=0.77$. j_L^* corresponds to j_{fd}^* . The factor f was also proposed in nearly its present form and values of 0.2 to 0.6 were found to be appropriate. Effects of geometry on the factors C and f were identified.

After extensive statistical study of the data, Battelle [6] concluded that different relations were needed for low flow, low subcooling and high flow, high subcooling ranges of the data. In the first range the modified Wallis correlation was used with

$$m = 0.213 - 0.226 \ln(j_{LIN}^*) \quad (A9)$$

$$C = 0.806 \left[(j_{LIN}^*) / 0.03 \right]^{(-0.008 + 0.328\lambda)} \quad (A10)$$

where j_{LIN}^* corresponds to j_{fin}^* .

In the latter range it was concluded that the modified Wallis correlation was unsatisfactory. The following relations were proposed:

$$j_L^* = j_{LIN}^* - f (j_g^* - j_{gcrit}^*)^2 \quad (A11)$$

$$j_{gcrit}^* = 0.19\lambda^{0.95} - 0.672\lambda [0.42 - j_{LIN}^*]^2 \quad (A12)$$

$$F = 1.32\lambda + 20.08 - (7.35\lambda - 0.94) j_{LIN}^* \quad (A13)$$

Early in 1976, Creare proposed the present correlation form in J^* parameters, Equations (3) to (5). The particular values of the coefficients were:

$$C = 0.32 \quad (A14)$$

$$m = \exp[-5.6 J_{fin}^*{}^{0.6}] \quad (A-15)$$

$$f = \left(\frac{P}{P_a}\right)^{\frac{1}{2}} \left[\frac{1}{1 + b J_{fin}^*}\right] \quad (A16)$$

where b was 16 for planar geometries and 30 for cylindrical geometries.

Later in 1976, Battelle [7] adopted a similar form but cast in j^* coordinates and based on K^* scaling.

$$[j_g^* - f \lambda j_{LIN}^*]^{\frac{1}{2}} + m [j_L^* / j_{LIN}^*]^{\frac{1}{2}} = [K / (D^*)^{\frac{1}{2}}] \quad (A17)$$

The values of $K=3.2$, $m=0.6932$ and $f=0.4198$ were proposed based on a linear regression analysis.

Shortly thereafter, Battelle [8] included additional data in the correlation and determined new values $K=3.2$, $\gamma=0.5687$, and $f=0.3202$. After evaluating over 20 correlation forms, Battelle [8] also modified their correlation to:

$$[j_g^* - f f_f \lambda j_{LIN}^*]^{\frac{1}{2}} + m m_f [j_L^* / j_{LIN}^*]^{\frac{1}{2}} = (K / (D^*)^{\frac{1}{2}})^{\frac{1}{2}} \quad (A18)$$

where m_f and f_f were the coefficients proposed by Creare. Deviation constants $m=2.1252$ and $f=0.90$ were proposed. Equation (A18) was shown to be a better correlation of the data than those derived previously because subcooling and j_{LIN}^* effects were better represented.

A further refinement was examined by Battelle [9] in which they compared Equation (A18) with the same equation replacing the right hand side by a constant C to achieve a form similar to the 1976 Creare correlation:

$$[j_g^* - f f_f \lambda j_{LIN}^*]^{\frac{1}{2}} + m m_f [j_L^* / j_{LIN}^*]^{\frac{1}{2}} = C \quad (A19)$$

Each equation was fit to available 1/15 and 2/15-scale Battelle data both independently and together. The rms deviations of the two correlation equations from the data were virtually identical. (This finding implied that the data analysis could not discriminate

between J^* and K^* scaling.) Battelle proposed that Equation (A18) continue to be used with coefficients $K=3.2$, $m=2.547$, and $f=1.231$.

Late in 1977 Battelle [10] proposed that the parameter trend coefficient should be modified to

$$m_f = \exp[-3.17(j_{LIN}^*)^{0.45}] \quad (A20)$$

$$f_f = \frac{1}{1 + 8.79 j_{LIN}^*} \quad (A21)$$

The change to f_f was significant because it amounted to dropping the previous dependence on pressure. They found that these changes reduced the rms deviation of the data correlation slightly. They also found that although the rms deviation of Equation (A19) was lower, Equation (A18) was superior in a statistical test of the correlation as representative of both 1/15 and 2/15 scale data. A need for a scale dependence different than j^* was identified.

Liu of Battelle [11] recently suggested the use of Equation (A19) but with the j^* parameters recast in terms of a new parameter I^* where:

$$I_g^* = j_g^* D^{1/8} \quad (A22)$$

This amounts to a compromise between j^* and K^* scaling.

Rothe et. al. [17] showed that saturated water data scales according to J^* in the range tested. They also pointed out that a constant value of m would be more appropriate for saturated water than the functional form $m(J_{LIN}^*)$ used previously. They identified large uncertainties associated with extrapolation of data to the complete bypass point and also with the use of subcooled water data to deduce saturated water behavior. These uncertainties are most obvious when the data are analyzed graphically, but also exist unseen when statistical analysis of the data is carried out numerically.

Recently, Battelle [12] recommended use of the J^* parameters in a new correlation:

$$[J_g^* - f_f \lambda J_{LIN}^*]^2 + m m_f [J_L^*/J_{LIN}^*]^2 = C \quad (A23)$$

where: $m_f = \exp[-6.79 J_{LIN}^*^{0.45}] \quad (A24)$

$$f_f = \frac{1}{1 + 47.78 J_{LIN}^*} \quad (A25)$$

$$C = 0.426 \quad (A26)$$

$$m = 6.49 \quad (A27)$$

$$f = 1.84 \quad (A28)$$

They continue to identify an undesirable scale dependence in comparing this correlation with separate data sets from 1/15-scale and 2/15-scale vessels.

In the present report we support the Battelle decision to drop the pressure term from the factor f and we propose significant further modifications based on new data for saturated water and for subcooled water over a broad range of pressures and subcoolings.

This history serves to show the very gradual progress being made on this topic. There has been a slow convergence of the Battelle and Creare correlations. Improvements to the correlations and the modeling of the physics have been mainly a result of new insights gained by acquisition and study of additional data taken under more controlled conditions or over a broader parameter range than earlier data.

APPENDIX A REFERENCES

- A-1) Wallis, G. B.; FLOODING VELOCITIES FOR AIR AND WATER IN VERTICAL TUBES; AEEW-R123, U.K.A.E.A., 1961.
- A-2) Wallis, G. B.; ONE-DIMENSIONAL TWO-PHASE FLOW; McGraw Hill Book Co., pp. 336-354, 1969.
- A-3) Pushkina, O. L. and Sorokin, U. L.; BREAKDOWN OF LIQUID FILM MOTION IN VERTICAL TUBES; Heat Transfer, Soviet Research Vol. 1, No. 5, pp. 56-64, September 1969.
- A-4) Wallis, G. B. and Makkenchery, S.; THE HANGING FILM PHENOMENON IN VERTICAL ANNULAR TWO-PHASE FLOW; ASME Journal of Fluids Engineering, pp. 297, 298, September 1974.
- A-5) Lovell, T. W.; THE EFFECT OF SCALE ON TWO-PHASE COUNTERCURRENT FLOW FLOODING IN VERTICAL TUBES; Thesis for Master of Science, Thayer School of Engineering, Dartmouth College, June 1977.
- A-6) Kuo, J. T. and Wallis, G. B.; THE BEHAVIOR OF GAS-LIQUID INTERFACES IN VERTICAL TUBES; Int. Journal of Multiphase Flow, Vol. 2, 521, 1976.
- A-7) A. E. Dukler and L. Smith; TWO PHASE INTERACTIONS IN CCF. STUDIES OF THE FLOODING MECHANISM, Summary Report No. 2, AT(49-24)-0194 University of Houston, December 30, 1977.
- A-8) Block, J. A. and Cary, C. N.; FLOW TOPOGRAPHIES IN STEAM/WATER COUNTERCURRENT FLOW; Presented at the ASME Winter Annual Meeting, San Francisco, 1978, Creare Technical Note TN-279.
- A-9) Block, J. A. and Crowley, C. J.; PRELIMINARY DATA AT 1/15-SCALE; Quarterly Progress Report, January 1 - March 31, 1976, Creare Technical Note TN-235, March 1976.
- A-10) Cudnik, R. A., et. al.; REACTOR SAFETY PROGRAM APPLICATIONS AND COORDINATION TASK 1, STEAM-WATER MIXING PROGRAM AND SYSTEM HYDRODYNAMICS; Quarterly Progress Report, BMI-NUREG-1962, November 1976.
- A-11) Carbiener, W. A.; STEAM WATER MIXING AND SYSTEM HYDRODYNAMICS PROGRAM; Battelle Columbus Laboratories, BMI-NUREG-1975; May 1977.
- A-12) Block, J. A. and Crowley, C. J.; EFFECT OF ELEVATED PRESSURE ON ECC DELIVERY IN A SIMULATED PWR GEOMETRY; Quarterly Progress Report, Creare Technical Note TN-224, October 1975.
- A-13) Block, J. A. and Wallis, G. B.; EFFECT OF HOT WALLS ON FLOW IN A SIMULATED PWR DOWNCOMER DURING A LOCA; Creare Technical Note TN-188, May 1974.
- A-14) Crowley, C. J. and Block, J. A.; LOWER PLENUM VOIDING WITH SCALED PWR PLENUM GEOMETRIES; Quarterly Progress Report, Creare Technical Note TN-258, May 1977.

APPENDIX B

COUNTERCURRENT FLOW DATA TABULATION

Countercurrent flow data reported here for the first time are listed in the following tables. This consists primarily of data at elevated pressure. The information provided in each table is:

TEST ID	-- identification numbers for each test
W_{gc}	-- countercurrent steam flow rate, lbm/sec
Q_{fd}	-- volumetric water flow rate delivered to lower plenum, gpm
Q_{fin}	-- volumetric water flow rate injected into cold legs, gpm
T_{ECC}	-- injected water temperature, $^{\circ}\text{F}$
ΔT_{SUB}	-- injected water subcooling, $^{\circ}\text{F}$
P_{LP}	-- lower plenum pressure, psia
P_c	-- discharge vessel pressure, psia
J_{fin}^*	-- dimensionless water flow rate injected
J_{gc}^*	-- dimensionless countercurrent steam flow
J_{fd}^*	-- dimensionless water flow rate delivered to lower plenum

Additional information which applies to these tables is:

Vessel scale - 1/15

Gap size - 0.5 in.

Average annulus circumference - 34.6 in.

Downcomer flow area - 0.12 ft^2

Plenum volume - 15.3 gal.

Broken leg diameter - 1.875 in. for Tables B1, B2, and B3

Broken leg diameter - 3.0 in. for Tables B4 and B5

TABLE B1
CCF DATA AT 30 PSIA

Test ID	W_{gc} (lbm/sec)	Q_{fd} (gpm)	Q_{fin} (gpm)	T_{ECC} (°F)	ΔT_{SUB} (°F)	P_{LP} (psia)	p_c (psia)	J^*_{fin}	J^*_{gc}	J^*_{fd}
2.0965	0.2022	65.5	60	82.5	163	25.6	14.5	0.1157	0.0838	0.1263
2.0966	0.3057	57.9	60	82.5	162	27.8	14.5	0.1157	0.1285	0.1117
2.0967	0.4046	48.3	60	79.5	163	26.8	14.5	0.1157	0.173	0.0931
2.0968	0.5074	46.5999	60	79.5	175	33.1	14.5	0.1157	0.1964	0.0899
2.0969	0.6046	6.1	60	80	177	34.8	14.5	0.1157	0.2286	0.0117
2.0970	0.5448	27.9	60	81	172	32.2	14.5	0.1157	0.2137	0.0538
2.0971	0.7089	0	60	82	169	31.2	14.5	0.1157	0.2822	0
2.0972	0.5712	29.5	60	82.5	171	32.4	14.5	0.1157	0.2234	0.0569
2.1133	0.5042	38.3	60	79.5	168	29.3	14.5	0.1157	0.2067	0.0738
2.1134	0.6082	31.9	60	79.5	168	29.7	14.5	0.1157	0.2477	0.0615
2.1135	0.7115	0	60	79.5	170	30.7	14.5	0.1157	0.2853	0
2.1136	0.658	6.3999	60	81	169	30.5	14.5	0.1157	0.2647	0.0123
2.1137	0.658	2.5999	60	79.5	170	30.7	14.5	0.1157	0.2639	0.005
2.1138	0.6253	2.5999	60	78.5	173	31.5	14.5	0.1157	0.2477	0.005
2.1139	0.6082	14.2	60	78.5	173	31.7	14.5	0.1157	0.2403	0.0273
2.1140	0.5042	38.3	60	78.5	168	29.1	14.5	0.1157	0.2073	0.0738
2.1141	0.412	56.9	60	78	166	27.9	14.5	0.1157	0.1728	0.1097
2.1142	0.4605	59	60	78	168	28.9	14.5	0.1157	0.1899	0.1138
2.1143	0.554	24	60	80	168	29.7	28.5	0.1157	0.2256	0.0463
2.11441	0.5817	37.0999	60	79.5	169	30	29	0.1157	0.2358	0.0715
2.11442	0.5817	44.9	60	79.5	169	30	29	0.1157	0.2358	0.0866
2.1145	0.5247	45.3	60	79.5	166	28.5	28.5	0.1157	0.2179	0.0874
2.1152	0.6082	4.3999	60	115	137	31.7	29.9	0.1157	0.2411	0.0084
2.11531	0.5042	24.5999	60	116.5	134	31	29.3	0.1157	0.202	0.0474
2.11532	0.5042	29	60	116.5	134	31	29.3	0.1157	0.202	0.0559
2.11541	0.554	50.0999	60	115.5	134	30.5	29.2	0.1157	0.2236	0.0966
2.11542	0.554	14.7	60	115.5	134	30.5	29.2	0.1157	0.2236	0.0283
2.1155	0.554	6.6	60	114	137	31.3	29.2	0.1157	0.2209	0.0127
2.1156	0.412	57.9	60	113	132	28	27.5	0.1157	0.1731	0.1117
2.1157	0.658	0	60	115.5	137	32.1	29.3	0.1157	0.2593	0
2.1158	0.6253	1.5	60	113.5	138	31.5	29.5	0.1157	0.2486	0.0028
2.11591	0.4605	51.0999	60	116.5	132	29.9	29.3	0.1157	0.1876	0.0985
2.11592	0.4605	12.7999	60	116.5	132	29.9	29.3	0.1157	0.1876	0.0246
2.1160	0.5247	16.5	60	116.5	134	31.2	29.3	0.1157	0.2096	0.0318
2.11611	0.4369	47.4	60	112.5	132	28.1	28.3	0.1157	0.1832	0.0914
2.11612	0.4369	30.7	60	112.5	132	28.1	28.3	0.1157	0.1832	0.0592
2.11621	0.4883	9.1	60	116.5	133	30.7	29.4	0.1157	0.1965	0.0175
2.11622	0.4883	17.2	60	116.5	133	30.7	29.4	0.1157	0.1965	0.0331
2.11631	0.4883	32.1999	60	114	136	30.7	35.3	0.1157	0.1965	0.0621
2.11632	0.4883	11.6	60	114	136	30.7	35.3	0.1157	0.1965	0.0223

TABLE B2
CCF DATA AT 45 PSIA

Test ID	W gc (lbw/sec)	Q _{fd} (gpm)	Q _{fin} (gpm)	T _{ECC} (°F)	ΔT _{SUB} (°F)	P _{LP} (psia)	p _c (psia)	J* _{fin}	J* _{gc}	J* _{fd}
2.1310	0.6749	4.0999	60	80	191	43.63	41.76	0.1157	0.2296	0.0079
2.1311	0.6879	4.0999	60	80	195	45.88	43.73	0.1158	0.2286	0.0079
2.1312	0.3899	76.6999	60	80	190	42.29	42.5	0.1157	0.1346	0.148
2.1313	0.4789	71.2999	60	80	191	43.09	43.96	0.1157	0.1639	0.1376
2.1314	0.5469	50.6999	60	80	191	43.3	41.3	0.1157	0.1867	0.0978
2.1315	0.5759	33.7999	60	80	192	44.04	45.12	0.1157	0.1951	0.0652
2.1316	0.6829	11.7999	60	80	192	43.9	43.27	0.1157	0.2317	0.0227
2.1317	0.6899	2.7999	60	80	191	43.55	42.52	0.1157	0.2349	0.0054
2.1318	0.618	32.2999	60	80	190	42.4	40.78	0.1157	0.213	0.0623
2.1319	0.6529	19.5	60	80	187	40.64	41.11	0.1157	0.2296	0.0376
2.1320	0.8.09	0.1999	60	80	193	44.92	43.01	0.1158	0.2822	0.0003
2.1321	0.9169	0	60	80	192	44.3	40.68	0.1158	0.3097	0
2.1322	0.8129	0.0999	60	80	191	43.42	39.31	0.1157	0.2772	0.0001
2.1323	0.7749	0.1999	60	80	191	43.48	41.54	0.1157	0.2641	0.0003
2.0973	0.6127	18.5	60	138	134	43.8	14.5	0.1158	0.2094	0.0357
2.0974	0.4046	50.1999	60	138.5	126	38.9	14.5	0.1157	0.1462	0.0968
2.0975	0.5074	20.7999	60	140	132	44.2	14.5	0.1158	0.1727	0.0401
2.0976	0.3057	56.9	60	139	135	45.6	14.5	0.1158	0.1025	0.1098
2.0977	0.2821	61.0999	60	139.5	134	45.2	14.5	0.1158	0.095	0.1179
2.0978	0.7555	0.6	60	140.5	139	49	14.5	0.1158	0.2451	0.0011
2.0979	0.8578	0	60	141	139	49.5	14.5	0.1158	0.277	0
2.11791	0.5042	30.9	60	139.5	134	44.7	44.1	0.1158	0.1707	0.0596
2.11792	0.5042	26.5	60	139.5	134	44.7	44.1	0.1158	0.1707	0.0511
2.1180	0.6082	1.9	60	139.5	134	45.3	44.1	0.1158	0.2047	0.0036
2.1181	0.554	5.8	60	139.5	135	45.9	44.5	0.1158	0.1852	0.0111
2.1182	0.5247	6.6999	60	139	136	46.3	44.7	0.1158	0.1747	0.0129
2.11831	0.412	51	60	139	133	44.3	44.7	0.1158	0.1401	0.0984
2.11832	0.412	29.4	60	139	133	44.3	44.7	0.1158	0.1401	0.0567
2.11841	0.4605	31.5999	60	139	135	45.3	44.9	0.1158	0.1549	0.0609
2.11842	0.4605	15.1	60	139	135	45.3	44.9	0.1158	0.1549	0.0291
2.1185	0.4229	45.5	60	139.5	133	44.5	45.1	0.1158	0.1482	0.0878
2.1186	0.357	53.9	60	139.5	134	44.9	45.3	0.1158	0.1206	0.104
2.1187	0.3093	48.1999	60	139.5	134	44.9	45.5	0.1158	0.1045	0.093
2.1188	0.2527	54.8	60	139.5	134	44.9	45.5	0.1158	0.0854	0.1057
2.1189	0.2065	54.8	60	139.5	134	44.9	45.7	0.1158	0.0697	0.1057
2.1190	0.5145	9.3999	60	139.5	136	46.1	45.1	0.1158	0.1717	0.0181
2.1191	0.7115	1	60	138.5	141	49.1	45.5	0.1158	0.2305	0.0019
2.1192	0.8141	2.4	60	138.5	135	45.1	41.1	0.1158	0.2744	0.0046
2.11941	0.5042	9.3999	60	140.5	133	45.1	44.5	0.1158	0.17	0.0181
2.11942	0.5042	13.2	60	140.5	133	45.1	44.5	0.1158	0.17	0.0254

TABLE B2 (continued)

CCF DATA AT 45 PSIA

Test ID	W_{gc} (lbm/sec)	Q_{fd} (gpm)	Q_{fin} (gpm)	T_{ECC} (°F)	ΔT_{SUB} (°F)	P_{LP} (psia)	P_c (psia)	J_{fin}^*	J_{gc}^*	J_{fd}^*
2.0943	0.5074	9.7	60	150.5	126	47.2	14.5	0.1158	0.1677	0.0187
2.0944	0.4046	40.3	60	151.5	115	40	14.5	0.1157	0.1445	0.0777
2.0945	0.3057	55	60	150.5	127	48.2	14.5	0.1158	0.1001	0.1061
2.0946	0.4453	18.0999	60	151	126	47.7	14.5	0.1158	0.1465	0.0349
2.0947	0.6589	0.6	60	151.5	129	50.4	14.5	0.1158	0.2113	0.0011
2.0948	0.264	55	60	152	126	48.1	14.5	0.1158	0.0865	0.1061
2.11951	0.5042	12.8999	60	149	121	42.7	41.7	0.1157	0.1746	0.0248
2.11952	0.5042	11.1	60	149	121	42.7	41.7	0.1157	0.1746	0.0214
2.1196	0.7115	1.5999	60	148	126	45.3	42.1	0.1158	0.2397	0.003
2.1197	0.3093	51.9	60	149	121	42.9	43.5	0.1157	0.1069	0.1001
2.11981	0.412	36.4	60	149.5	122	43.5	43.3	0.1158	0.1415	0.0702
2.11982	0.412	18.5	60	149.5	122	43.5	43.3	0.1158	0.1415	0.0357
2.11991	0.4605	7.0699	60	149.5	123	44.5	43.5	0.1158	0.1564	0.0136
2.11992	0.4605	13.2	60	149.5	123	44.5	43.5	0.1158	0.1564	0.0254
2.1200	0.2065	61.099	60	149.5	122	43.9	43.7	0.1158	0.0706	0.1179
2.1201	0.2527	57.9	60	148.5	122	43.1	43.7	0.1157	0.0871	0.1117
2.12021	0.4369	17.7999	60	148.5	122	43.1	43.1	0.1157	0.1507	0.0343
2.12022	0.4369	15.7	60	148.5	122	43.1	43.1	0.1157	0.1507	0.0303
2.1203	0.6082	1.5	60	149.5	124	45.1	43.3	0.1158	0.2054	0.0028
2.1204	0.357	37.0999	60	150.5	120	43.1	43.3	0.1157	0.1231	0.0716
2.1205	0.8141	0.3999	60	151	125	47.1	44.1	0.1158	0.2694	0.0007
2.0949	0.3057	45.8	60	208.5	71	49.2	14.5	0.1158	0.1002	0.0884
2.0950	0.264	39.0999	60	211	64	46.3	14.5	0.1158	0.089	0.0754
2.0951	0.2012	56.9	60	210.5	64	46	14.5	0.1158	0.0684	0.1098
2.0952	0.178	56.9	60	210	65	46.4	14.5	0.1158	0.0532	0.1098
2.0953	0.4046	5.5	60	209.5	73	51.3	14.5	0.1158	0.1301	0.0106
2.0954	0.3453	6.6	60	209.5	67	47.3	14.5	0.1158	0.1153	0.0127
2.0955	0.3153	12.2	60	209.5	67	47.3	14.5	0.1158	0.1052	0.0235
2.0956	0.6589	0.3	60	208.5	78	55.1	14.5	0.1158	0.2048	0.0005
2.1095	0.4115	4.6	60	213	65	48.2	14.5	0.1158	0.1363	0.0088
2.1096	0.5091	1.7	60	213.5	66	49.2	14.5	0.1158	0.167	0.0032
2.1097	0.6093	0	60	214	65	49.2	14.5	0.1150	0.1999	0
2.1098	0.5514	0	60	214	62	46.6	14.5	0.1158	0.1855	0
2.1099	0.4568	1.5999	60	214.5	57	43.9	14.5	0.1158	0.1581	0.003

TABLE B3
CCF DATA AT 65 PSIA

Test ID	w_{gc} (lbm/sec)	Q_g (gpm)	Q_{fin} (gpm)	T_{BCC} (°F)	ΔT_{SUB} (°F)	p_{LP} (psia)	p_c (psia)	J^*_{fin}	J^*_{gc}	J^*_{fd}
2.1284	0.7487	36	60	79.5	222	68.5	66.7	0.1158	0.2065	0.0695
2.1285	0.8185	33.9	60	80.5	220	67.1	64.7	0.1158	0.2279	0.0654
2.1286	0.9211	1.2999	60	80.5	221	68.5	64.5	0.1158	0.254	0.0025
2.1287	0.9639	0.5	60	80	219	65.5	61.7	0.1158	0.2714	0.0009
2.1269	1.0048	0.5	60	80	218	64.5	61.3	0.1158	0.2849	0.0009
2.1290	1.0439	0.5	60	80	217	63.9	59.9	0.1158	0.2973	0.0009
2.1291	1.1877	0.3	60	80.5	219	66.5	61.9	0.1158	0.3321	0.0005
2.1292	0.6837	39.6999	60	80	220	66.9	65.5	0.1158	0.1906	0.0766
2.1293	0.6082	55	60	78.5	220	65.3	64.5	0.1158	0.1715	0.1061
2.1294	0.621	53.0999	60	79	222	67.5	66.3	0.1158	0.1724	0.1025
2.1295	0.676	55	60	79.5	218	64.1	63.5	0.1158	0.1923	0.1061
2.1296	0.838	26.5	60	79.5	220	66.3	62.5	0.1158	0.2346	0.0511
2.1297	0.8442	3.8	60	81	218	65.9	62.1	0.1158	0.237	0.0073
2.11641	0.6082	47.4	60	130.5	169	65.9	66.3	0.1158	0.1717	0.0915
2.11642	0.6082	22.4	60	130.5	169	65.9	66.3	0.1158	0.1717	0.0432
2.11651	0.5042	55.9	60	130	167	64.3	65.3	0.1158	0.1439	0.1079
2.11652	0.5042	27.9	60	130	167	64.3	65.3	0.1158	0.1439	0.0538
2.1166	0.4605	48.3	60	129.5	168	64.3	65.7	0.1158	0.1314	0.0932
2.1167	0.412	50.0999	60	128.5	169	64.3	65.7	0.1158	0.1176	0.0967
2.11681	0.7115	19.9	60	129.5	170	66.1	65.9	0.1158	0.2005	0.0384
2.11682	0.7115	8.8999	60	129.5	170	66.1	65.9	0.1158	0.2005	0.0171
2.11691	0.658	10.2999	60	130	169	65.7	65.7	0.1158	0.186	0.0198
2.11692	0.658	17.9	60	130	169	65.7	65.7	0.1158	0.186	0.0345
2.1170	0.658	3.9	60	130	169	65.7	65.3	0.1158	0.186	0.0075
2.11711	0.7115	1.7999	60	132	168	66.9	65.9	0.1158	0.1995	0.0034
2.11712	0.7115	4.8999	60	132	168	66.9	65.9	0.1158	0.1995	0.0094
2.1172	0.6253	8.3999	60	130.5	168	65.3	65.3	0.1158	0.1772	0.0162
2.11731	0.6082	37	60	129.5	168	64.5	65.3	0.1158	0.1734	0.0714
2.11732	0.6082	26.5	60	129.5	168	64.5	65.3	0.1158	0.1734	0.0511
2.11741	0.6253	36.1999	60	130.5	167	64.7	65.1	0.1158	0.178	0.0698
2.11742	0.6253	26.0999	60	130.5	167	64.7	65.1	0.1158	0.178	0.0503
2.11751	0.8141	6.3	60	130.5	167	64.3	64.1	0.1158	0.2324	0.0121
2.11752	0.8141	4.8	60	130.5	167	64.3	64.1	0.1158	0.2324	0.0092
2.1176	0.8576	3.8	60	130.5	167	64.3	64.3	0.1158	0.2449	0.0073
2.1177	0.9548	0.6	60	130.5	168	65.5	63.9	0.1158	0.2703	0.0011
2.1178	1.0124	0.8999	60	129.5	170	66.3	63.7	0.1158	0.2849	0.0017

TABLE B3 (continued)

CCF DATA AT 65 PSIA

Test ID	W_{gc} (lbm/sec)	Q_f (gpm)	Q_{fin} (gpm)	T_{ECC} (°F)	ΔT_{SUB} (°F)	P_{LP} (psia)	p_c (psia)	J_{fin}^*	J_{gc}^*	J_{fd}^*
2.0982	0.5074	11.8999	60	162.5	133	62.5	14.5	0.1158	0.1475	0.0229
2.0984	0.4341	42.1999	60	165.5	132	64.7	14.5	0.1158	0.1242	0.0814
2.0985	0.4563	18.7	60	165.5	130	62.3	14.5	0.1158	0.1329	0.0361
2.0986	0.6046	5.6	60	165.5	131	63.8	14.5	0.1158	0.1742	0.0108
2.0987	0.7555	1.2	60	166.5	134	67.5	14.5	0.1158	0.212	0.0023
2.0988	0.4046	47.4	60	166.5	132	65.1	14.5	0.1158	0.1155	0.0915
2.0989	0.3453	61.0999	60	167.5	129	63.5	14.5	0.1158	0.0997	0.1179
2.12061	0.6253	13.8999	60	162.5	134	63.3	62.3	0.1158	0.1807	0.0268
2.12062	0.6253	6.8999	60	162.5	134	63.3	62.3	0.1158	0.1807	0.0133
2.12071	0.412	42.5	60	161.5	133	61.7	63.1	0.1158	0.1205	0.082
2.12072	0.412	25.7999	60	161.5	133	61.7	63.1	0.1158	0.1205	0.0498
2.1208	0.3093	42.5	60	161.5	136	63.9	65.5	0.1158	0.089	0.082
2.1209	0.2527	54	60	162	135	63.9	65.1	0.1158	0.0727	0.1042
2.1210	0.357	47.5999	60	162	135	63.9	65.1	0.1158	0.1027	0.0919
2.12111	0.5042	16	60	162	135	63.9	64.5	0.1158	0.145	0.0308
2.12112	0.5042	13.6	60	162	135	63.9	64.5	0.1158	0.145	0.0262
2.1212	0.7115	0.3	60	160.5	140	66.9	65.9	0.1158	0.2003	0.0005
2.12131	0.4605	26.5	60	162.5	135	64.5	65.7	0.1158	0.1319	0.0510
2.12132	0.4605	19.2999	60	162.5	135	64.5	65.7	0.1158	0.1319	0.0371
2.1214	0.658	1.5999	60	164	136	66.9	65.9	0.1158	0.1853	0.003
2.1084	0.3682	52	60	214	82	63.2	14.5	0.1158	0.1075	0.1003
2.1085	0.2815	53.9	60	212.5	85	64	14.5	0.1158	0.0817	0.104
2.1086	0.238	52	60	213	84	63.9	14.5	0.1158	0.0691	0.1003
2.1087	0.2021	53.9	60	213	84	63.8	14.5	0.1158	0.0587	0.104
2.1088	0.1685	54.9	60	213.5	83	63.6	14.5	0.1158	0.049	0.1059
2.1089	0.5091	13.5	60	214	85	65.7	14.5	0.1158	0.146	0.026
2.1090	0.4568	9.1	60	211	87	65.2	14.5	0.1158	0.1314	0.0175
2.1091	0.4115	25.0999	60	211.5	86	64.5	14.5	0.1158	0.119	0.0484
2.1092	0.6621	1.0999	60	212	91	69.3	14.5	0.1158	0.1852	0.0021
2.1093	0.6093	4.5	60	212.5	85	64	14.5	0.1158	0.1768	0.0086
2.1094	0.7108	0	60	213	90	69.3	14.5	0.1158	0.1988	0

TABLE B4
SATURATED ECC CCF DATA AT ELEVATED PRESSURE (ENLARGED BREAK)

Test ID	W_{gc} (lbm/sec)	Q_{fd} (gpm)	Q_{fin} (gpm)	T_{ECC} (°F)	ΔT_{SUB} (°F)	p_{LP} (psia)	p_c (psia)	J_{fin}^*	J_{gc}^*	J_{fd}^*
2.1354	0.1021	54.8	60	243.5	3	29.1	28.9	0.1157	0.0431	0.1057
2.1355	0.1123	52.9	60	243.5	4	29.7	29.3	0.1157	0.047	0.102
2.1356	0.1771	12	60	245	6	31.5	30.3	0.1157	0.0721	0.0231
2.1357	0.1516	19.2999	60	245	6	31	30.3	0.1157	0.0622	0.0372
2.1358	0.2516	5.5	60	246.5	8	33.1	31.1	0.1157	0.1001	0.0106
2.1359	0.5599	0.6	60	245	16	36.7	30.9	0.1157	0.2121	0.0011
2.1360	0.0862	57.9	60	243.5	6	30.3	29.8	0.1157	0.0357	0.1117
2.1361	0.1371	39	60	243.5	8	31.7	31	0.1157	0.0556	0.0752
2.1362	0.3853	1.9	60	243.5	14	35	30.3	0.1157	0.1492	0.0036
2.1363	0.453	1.2999	60	246.5	13	36.1	30.5	0.1157	0.173	0.0025
2.1347	0.1407	52.9	60	290.5	10	67.1	66.7	0.1158	0.0407	0.1021
2.1348	0.2827	18.0999	60	295	7	68.1	66.9	0.1158	0.0813	0.0349
2.1349	0.2188	25.5	60	293.5	8	67.9	67.1	0.1158	0.063	0.0492
2.1350	0.3774	5.1	60	290.5	11	67.9	65.9	0.1158	0.1086	0.0098
2.1351	0.5482	1.9	60	290	12	68.9	65.7	0.1158	0.1567	0.0036
2.1352	0.6899	1.2999	60	296	9	72	67.5	0.1158	0.1935	0.0025
2.1353	0.4716	3.1999	60	295.5	8	70.3	68.5	0.1158	0.1337	0.0061

TABLE B5
SUBCOOLED CCF DATA AT LOW PRESSURE (ENLARGED BREAK)

Test ID	\dot{W}_{gc} (lbm/sec)	\dot{Q}_{fd} (gpm)	\dot{Q}_{fin} (gpm)	T_{ECC} (°F)	ΔT_{SUB} (°F)	P_{LP} (psia)	P_c (psia)	J_{fin}^*	J_{gc}^*	J_{fd}^*
2.0894	0.3057	27	30	77	135	15.1	14.5	0.0578	0.1713	0.052
2.0895	0.3453	4.1	30	77	135	15.2	14.5	0.0578	0.1929	0.0079
2.0896	0.3231	10.5	30	77.5	135	15.3	14.5	0.0578	0.1799	0.0202
2.0897	0.3153	25.0999	30	78.5	133	15	14.5	0.0578	0.1773	0.0484
2.0898	0.2908	32.1999	30	78.5	133	14.9	14.5	0.0578	0.1641	0.0621
2.0899	0.2992	29.5	30	79.5	132	15	14.5	0.0578	0.1683	0.0569
2.0900	0.4046	2.8	30	80	133	15.5	14.5	0.0578	0.224	0.0054
2.0901	0.4563	0	30	81	133	16	14.5	0.0578	0.2488	0
2.0778	0.4563	0	60	80	139	17.4	14.5	0.1157	0.2391	0
2.0779	0.3057	55.4	60	82	132	15.8	14.5	0.1157	0.1678	0.1068
2.0780	0.4046	39.0999	60	81.5	132	15.6	14.5	0.1157	0.2234	0.0754
2.0781	0.4284	16.2999	60	82.5	132	15.9	14.5	0.1157	0.2343	0.0314
2.0782	0.4453	1.2999	60	82	132	16	14.5	0.1157	0.2429	0.0025
2.0783	0.3453	40.5999	60	81	131	15.4	14.5	0.1157	0.1918	0.0783
2.0784	0.2732	60	60	82	130	14.9	14.5	0.1157	0.1542	0.1157
2.0785	0.3453	46.4	60	80	133	15.6	14.5	0.1157	0.1906	0.0895
2.0786	0.4341	0	60	81.5	133	15.9	14.5	0.1157	0.2375	0
2.0787	0.4284	3.5999	60	81.5	132	15.6	14.5	0.1157	0.2365	0.0069
2.0788	0.4167	6.3999	60	81	133	15.9	14.5	0.1157	0.2279	0.0123
2.0789	0.4226	5.5	60	82.5	133	16.3	14.5	0.1157	0.2285	0.0106
2.0790	0.4046	17.0999	60	82.5	134	16.8	14.5	0.1157	0.2157	0.0329
2.0902	0.3453	56.4	60	77	135	14.8	14.5	0.1157	0.1955	0.1087
2.0903	0.4046	27.5	60	78	135	15.5	14.5	0.1157	0.224	0.053
2.0904	0.4563	3	60	78.5	135	15.7	14.5	0.1157	0.251	0.0057
2.0905	0.4226	32.1999	60	80	132	15.1	14.5	0.1157	0.2369	0.0621
2.0906	0.3057	53	60	82	130	14.9	14.5	0.1157	0.1726	0.1022
2.0907	0.2908	57.9	60	82.5	129	14.8	14.5	0.1157	0.1647	0.1116
2.0908	0.5074	0	60	83.5	131	16	14.5	0.1157	0.2768	0
2.0909	0.4226	12.7	60	84	130	15.8	14.5	0.1157	0.2319	0.0244

NRC FORM 335 (7-77)		U.S. NUCLEAR REGULATORY COMMISSION BIBLIOGRAPHIC DATA SHEET		1. REPORT NUMBER (Assigned by DDC) NUREG/CR-0464	
4. TITLE AND SUBTITLE (Add Volume No., if appropriate) Scaling of Pressure and Subcooling for Countercurrent Flow				2. (Leave blank)	
7. AUTHOR(S) P.H. Rothe and C.J. Crowley				5. DATE REPORT COMPLETED	
9. PERFORMING ORGANIZATION NAME AND MAILING ADDRESS (Include Zip Code) CREARE, Inc. Hanover, New Hampshire 03755				MONTH YEAR October 1978	
				DATE REPORT ISSUED	
12. SPONSORING ORGANIZATION NAME AND MAILING ADDRESS (Include Zip Code) Office of Nuclear Regulatory Research U.S. Nuclear Regulatory Commission Washington, D.C. 20555				MONTH YEAR November 1978	
				6. (Leave blank)	
				8. (Leave blank)	
				10. PROJECT/TASK/WORK UNIT NO.	
				11. CONTRACT NO. NRC-04-75-162	
13. TYPE OF REPORT Quarterly Progress			PERIOD COVERED (Inclusive dates) April 1, 1978 - June 30, 1978		
15. SUPPLEMENTARY NOTES				14. (Leave blank)	
16. ABSTRACT (200 words or less) Recent results of a continuing program to develop semi-empirical models of lower plenum filling after a hypothetical PWR LOCA are presented. The idealized situation of countercurrent flow in a 1/15-scale PWR model is specifically addressed here. For saturated water behavior in small-scale facilities, it is shown that the dimensionless J^* parameters properly scale the effects of vessel size, injection rate, and (for the first time with steam and water) vessel pressure. Building on previous work, new correlation concepts are proposed to account for the effects of condensation on ECC bypass. Comparison with new data over an increased range of pressures and subcoolings shows that for a given injection rate, the effects of condensation can be accounted solely in terms of thermodynamic ratio rather than pressure or subcooling independently. The data indicate that subcooling has a weaker effect on ECC bypass than was previously believed. The data also reveal a transition in behavior at a thermodynamic ratio near unity; at values below this transition the behavior is close to that of saturated water at all pressures tested. These findings suggest a need for caution when taking credit for the benefits of subcooling on ECC bypass in calculated LOCA transients.					
17. KEY WORDS AND DOCUMENT ANALYSIS			17a. DESCRIPTORS		
17b. IDENTIFIERS/OPEN-ENDED TERMS					
18. AVAILABILITY STATEMENT Unlimited			19. SECURITY CLASS (This report)		21. NO. OF PAGES
			20. SECURITY CLASS (This page)		22. PRICE \$

UNITED STATES
NUCLEAR REGULATORY COMMISSION
WASHINGTON, D. C. 20555

OFFICIAL BUSINESS
PENALTY FOR PRIVATE USE, \$300

POSTAGE AND FEES PAID
U.S. NUCLEAR REGULATORY
COMMISSION

